Widely-Linear Equalization and Blind Channel Identification For Interference-Contaminated Multicarrier Systems

Donatella Darsena, Giacinto Gelli, *Member, IEEE*, Luigi Paura, and Francesco Verde

***Abstract*— This paper addresses the problem of designing efficient detection techniques for multicarrier transmission systems operating in the presence of narrowband interference (NBI). In this case, conventional linear receivers, such as the zero-forcing (ZF) or the minimum-mean square error (MMSE) ones, usually perform poorly, since they are not capable of suppressing satisfactorily the NBI. To synthesize interference-resistant detection algorithms, we resort to widely-linear (WL) filtering, which allows one to exploit the noncircularity property of the desired signal constellation by jointly processing the received signal and its complex-conjugate version. In particular, we synthesize new WL-ZF receivers for multicarrier systems, which mitigate, in the minimum output-energy (MOE) sense, the NBI contribution at the receiver output, without requiring knowledge of the NBI statistics. By exploiting the noncircularity property, we also propose a new subspace-based blind channel identification algorithm, and derive the channel identifiability condition. Blind identification can be performed satisfactorily also in the presence of NBI, requiring only an approximate rank determination of the NBI autocorrelation matrix. The performance analysis shows that the proposed MOE WL-ZF receiver, even when implemented blindly, assures a substantial improvement over the conventional linear ZF and MMSE ones, particularly when the NBI bandwidth is very small in comparison with the intercarrier spacing and the NBI is not exactly located on a subcarrier.**

***Index Terms*— Widely-linear filtering, multicarrier systems, noncircular constellations, equalization, blind channel identification.**

I. INTRODUCTION

IN recent years, a great bulk of research activities have tackled the problem of designing efficient detection techniques for both wireline and wireless multicarrier transmission systems, such as discrete multitone (DMT), orthogonal frequency-division multiplexing (OFDM) and multicarrier code-division multiple-access (MC-CDMA) systems. Multicarrier schemes belong to the family of *block-oriented* transmission techniques, which counteract intersymbol interference [referred in this context to as *interblock interference* (IBI)] more efficiently than single-carrier ones, by reducing the symbol rate and inserting a cyclic prefix (CP) at the transmitter side [36]. Besides the obvious increase of latency, a drawback of block-oriented systems is the rising of *intercarrier interference* (ICI), which however can be controlled and even eliminated by careful system design. As a matter of fact, under the assumption that the CP length exceeds the channel dispersion, the conventional linear *zero-forcing* (ZF) (i.e., no IBI and ICI) receiver [36] allows one to recover the transmitted symbols, after CP removal, by means of the computationally-efficient fast Fourier transform (FFT) algorithm, followed by one-tap frequency-domain equalization (FEQ).

In many applications, however, broadband multicarrier systems are expected to cope with narrowband interference (NBI). This happens in wireless systems, when they operate in the presence of narrowband communication systems (e.g., overlay systems or systems transmitting in non-licensed bands), or in wireline ones, wherein the transmission cables might be exposed to crosstalk or radio-frequency interference. In these scenarios, the conventional ZF receiver might perform poorly, since no specific measure is undertaken to counteract the NBI effects. To synthesize interference-resistant detection algorithms, if the channel is quasi-stationary and channel-state information is available at the transmitter, a sensible approach is to perform joint transmitter-receiver optimization [29], [30] or simple bit/power loading [28], which is a standard procedure in point-to-point wireline multicarrier systems (e.g., xDSL systems). However, in packet-oriented wireless applications, the relatively fast channel variations usually prevent such an approach from being useful, and one is forced to concentrate exclusively on receiver optimization. By focusing on the class of linear receivers, a detailed mathematical formulation of the problem (see Section III) shows that imposing the ZF constraint and removing the entire CP consumes all the available degrees of freedom in the synthesis of the receiver, leading to the *unique* solution represented by the conventional receiver (i.e., FFT followed by FEQ). To gain some degrees of freedom for NBI suppression, one can renounce to the ZF constraint and synthesize instead the minimum-mean square-error (MMSE) receiver, which, however, does not assure satisfactory performance in most interference-contaminated scenarios (see simulations in Section VI).

To overcome the above-mentioned limitations and gain additional degrees of freedom, a possible solution consists of increasing the dimensionality of the observation space, which can be achieved, for example, by processing also the

Manuscript received ....; revised .....and....

Some results of this paper were presented at the 6th Baiona Workshop on Signal Processing in Communications, Baiona (Spain), September 2003.

This work was supported by the MIUR 2002 Italian National Research Project (PRIN 2002).

The authors are with Dipartimento di Ingegneria Elettronica e delle Telecomunicazioni, Università di Napoli Federico II, via Claudio 21, I-80125, Napoli, Italy [tel: +39-0817683154, fax: +39-0817683149, e-mail: (darsena, gelli, paura, f.verde)@unina.it].

Publisher Item Identifier S 0000-0000(00)00000-3.

entire CP [7] or a portion thereof [18], by oversampling the received signal [26], or by employing multiple antennas at the receiver side [17], all of which entail increased computational requirements. Alternatively, IBI, ICI, and NBI effects could be counteracted by inserting zeros at the transmitter (so called *zero-padding* systems [29], [30], [20]) instead of using a CP, which moreover assures equalization of finite-impulse response (FIR) channels regardless of the channel zero locations, but is not compatible with existing standards (e.g., IEEE 802.11a and HIPERLAN/2), which resort to the CP solution.

In this paper, we focus on the receiver synthesis for CP-based multicarrier systems and, to gain additional degrees of freedom for receiver optimization, we exploit the *noncircularity* [23] property exhibited by many signal constellations in digital communications. Such an approach has been first proposed in the framework of single-carrier communication systems, with particular reference to code-division multiple-access (CDMA) systems [34], leading to the synthesis of *widely-linear* (WL) [24] receivers, which jointly elaborate the received signal and its conjugate version, to mitigate the effects of NBI [9], or to improve the suppression of both multiple-access interference (MAI) and NBI with simple [10] and iterative [16] schemes. Other recent contributions employing the WL approach are in the area of channel equalization [11] and in space-time coded systems [12]. In the multicarrier context, however, applications of the noncircularity property are limited to the area of synchronization (see works [4], [5] on frequency-offset estimation), and its application to improve the receiver performance has not, to the best of our knowledge, been already explored. In this paper, we apply the WL approach to devise new WL-ZF receivers, which, by exploiting the noncircularity property, are able to gain the additional degrees of freedom needed to mitigate, in the minimum output-energy (MOE) [14] sense, the effects of the NBI at the receiver output.

The exploitation of the noncircularity property is also proposed in this paper for achieving *blind* channel identification for multicarrier systems, i.e., without requiring the use of training symbols or pilot tones. Some recent works in this field borrow concepts from the well-established area of subspace-based blind equalization for single-carrier systems [19], which exploits the subspace properties of the autocorrelation matrix of the received data to blindly estimate the channel (up to a complex scalar). A blind technique for OFDM systems, recently proposed in [26], works for a system *without* CP, by resorting to oversampling and/or multiple antennas at the receiver. The same authors proposed in [27] another subspace-based method, which can be applied to a system with CP, by exploiting the presence of *virtual* carriers (i.e., unused carriers, a solution present in several multicarrier standards). In order to build an autocorrelation matrix, whose subspace properties allow one to estimate the channel, another technique [21] for OFDM systems with CP consists of stacking *two* consecutive OFDM received symbols (including the CP). In this paper, we take a different approach, more specifically, in order to exploit the noncircularity property, we build an *augmented* received vector by stacking the received symbol and its complex conjugate (without CP), whose autocorrelation matrix allows one to blindly estimate the channel (up to a *real* scalar). We also derive the channel identifiability conditions, which show that only channels exhibiting a particular symmetry between the zeros are not identifiable by the proposed approach. However, simulation results show that the performance of the proposed identification method does not excessively degrade when the channel zeros configuration is close to exhibit such a symmetry.

The paper is organized as follows. In Section II, we introduce the multicarrier system model and discuss the assumptions that hold throughout the paper. In Section III, the synthesis of ZF linear receivers is discussed: although most of the related theory is well established, our treatment allows us to pinpoint some key issues that are not widely recognized in the literature, and will serve as a starting point in Section IV for deriving new WL-ZF receivers for multicarrier systems. In Section V, we present the new blind channel identification algorithm. Section VI provides numerical results, obtained either analytically or by Monte Carlo simulations, aimed at assessing the performances of the proposed equalization and channel identification algorithms. Concluding remarks are drawn in Section VII.

II. The multicarrier system model

In the rest of the paper, we use the following notations and terminology. Matrices [vectors] are denoted with upper case [lower case] boldface letters (e.g., $\boldsymbol{A}$ or $\boldsymbol{a}$); the field of $m \times n$ complex [real] matrices is denoted as $\mathbb{C}^{m\times n}$ [$\mathbb{R}^{m\times n}$], with $\mathbb{C}^m$ [$\mathbb{R}^m$] used as a shorthand for $\mathbb{C}^{m\times 1}$ [$\mathbb{R}^{m\times 1}$]; $\{\boldsymbol{A}\}_{ij}$ indicates the $(i+1, j+1)$th element of matrix $\boldsymbol{A} \in \mathbb{C}^{m\times n}$, with $i \in \{0, 1, \ldots, m-1\}$ and $j \in \{0, 1, \ldots, n-1\}$; a tall matrix $\boldsymbol{A}$ is a matrix with more rows than columns; the superscripts $*$, T, H, -1, and $\dagger$ denote the conjugate, the transpose, the hermitian (conjugate transpose), the inverse, and the Moore-Penrose generalized inverse (pseudo-inverse) of a matrix, respectively; $\mathbf{0}_m \in \mathbb{R}^m$ denote the null vector, $\mathbf{O}_{m\times n} \in \mathbb{R}^{m\times n}$ the null matrix, and $\mathbf{I}_m \in \mathbb{R}^{m\times m}$ the identity matrix; trace$(\cdot)$ and det$(\cdot)$ represent the trace and the determinant; range$(\boldsymbol{A})$ and range$^{\perp}(\boldsymbol{A})$ denote the column space of $\boldsymbol{A} \in \mathbb{C}^{m\times n}[\mathbb{R}^{m\times n}]$ and its orthogonal complement in $\mathbb{C}^m[\mathbb{R}^m]$; $\langle \boldsymbol{A}, \boldsymbol{B}\rangle \triangleq \text{trace}(\boldsymbol{A}\,\boldsymbol{B}^H)$ denote the scalar product in $\mathbb{C}^{m\times n}$ and $\|\boldsymbol{A}\| \triangleq [\text{trace}(\boldsymbol{A}\boldsymbol{A}^H)]^{\frac{1}{2}}$ the induced (Frobenius) norm; vec$(\boldsymbol{A}) \in \mathbb{C}^{mn}$ denote the (column) vector obtained by concatenating the columns of $\boldsymbol{A} \in \mathbb{C}^{m\times n}$; finally, E$[\cdot]$ denotes ensemble averaging, $\star$ convolution, and δ_k the Kronecker delta, i.e., $\delta_k = 1$ for $k = 0$, otherwise it is zero.

Let us consider a multicarrier system with M subcarriers, wherein the data stream $\{s(n)\}_{n\in\mathbb{Z}}$ at rate $1/T$ is converted at the transmitter side into M parallel substreams $s_m(n) \triangleq s(nM+m)$, $m = 0, 1, \ldots, M-1$. For each value of $n \in \mathbb{Z}$, the sequence $\{s_m(n)\}_{m=0}^{M-1}$ is subject to the inverse discrete Fourier transform (IDFT) with respect to (w.r.t.) m, thus, obtaining the sequence $\widetilde{u}_p(n) = \frac{1}{\sqrt{M}} \sum_{m=0}^{M-1} s_m(n)\, e^{j\frac{2\pi}{M}mp}$, for $p \in \{0, 1, \ldots, M-1\}$. The IDFT can be compactly expressed in matrix-vector notation by introducing the column vectors $\widetilde{\boldsymbol{u}}(n) \triangleq [\widetilde{u}_0(n), \widetilde{u}_1(n), \ldots, \widetilde{u}_{M-1}(n)]^T \in \mathbb{C}^M$ and

$\boldsymbol{s}(n) \triangleq [s_0(n), s_1(n), \ldots, s_{M-1}(n)]^T \in \mathbb{C}^M$, as $\widetilde{\boldsymbol{u}}(n) = \boldsymbol{W}_{\text{IDFT}}\, \boldsymbol{s}(n)$, where $\{\boldsymbol{W}_{\text{IDFT}}\}_{mp} \triangleq \frac{1}{\sqrt{M}} e^{j \frac{2\pi}{M} mp}$, $m, p \in \{0, 1, \ldots, M-1\}$, is the unitary symmetric IDFT matrix, and its inverse $\boldsymbol{W}_{\text{DFT}} \triangleq \boldsymbol{W}_{\text{IDFT}}^{-1} = \boldsymbol{W}_{\text{IDFT}}^H$ defines the discrete Fourier transform (DFT). In order to counteract the temporal dispersion induced by the channel, a CP, built from the last $0 < L_{\text{cp}} < M$ samples of $\widetilde{\boldsymbol{u}}(n)$, is inserted at the beginning of the IDFT block $\widetilde{\boldsymbol{u}}(n)$, obtaining thus the new vector $\boldsymbol{u}(n) \triangleq [u_0(n), u_1(n), \ldots, u_{P-1}(n)]^T = [\widetilde{u}_{M-L_{\text{cp}}}(n), \ldots, \widetilde{u}_{M-1}(n), \widetilde{u}_0(n), \ldots, \widetilde{u}_{M-1}(n)]^T \in \mathbb{C}^P$, with $P \triangleq M + L_{\text{cp}}$. The CP insertion can be described in matrix terms as

$$\boldsymbol{u}(n) = \boldsymbol{T}_{\text{cp}}\, \widetilde{\boldsymbol{u}}(n) = \boldsymbol{T}_{\text{cp}}\, \boldsymbol{W}_{\text{IDFT}}\, \boldsymbol{s}(n) = \boldsymbol{T}_0\, \boldsymbol{s}(n)\,, \quad (1)$$

where $\boldsymbol{T}_{\text{cp}} \triangleq [\mathbf{I}_{\text{cp}}^T, \mathbf{I}_M]^T \in \mathbb{R}^{P \times M}$, with $\mathbf{I}_{\text{cp}} \in \mathbb{R}^{L_{\text{cp}} \times M}$ obtained from $\mathbf{I}_M$ by picking its last L_{cp} rows, and $\boldsymbol{T}_0 \triangleq \boldsymbol{T}_{\text{cp}} \boldsymbol{W}_{\text{IDFT}} \in \mathbb{C}^{P \times M}$ is the *precoding* matrix. Vector $\boldsymbol{u}(n)$ undergoes parallel-to-serial (P/S) conversion, and the resulting sequence $\{u(n)\}_{n \in \mathbb{Z}}$, defined by $u(nP + p) = u_p(n)$, $p \in \{0, 1, \ldots, P-1\}$, feeds a digital-to-analog converter (DAC), operating at rate $1/T_c = P/T$, where T_c is the sampling period. The continuous-time signal at the output of the DAC can be expressed as $u_c(t) = \sum_{k=-\infty}^{+\infty} \sum_{p=0}^{P-1} u_p(k)\, \psi_c(t - p\,T_c - k\,T)$, where $\psi_c(\tau)$ denotes the impulse response of the DAC interpolator. After up-conversion, the transmitted signal propagates through a physical channel modeled as a linear time-invariant (LTI) filter, whose impulse response is $g_c(\tau)$. If we denote with $\phi_c(\tau)$ the impulse response of the (anti-aliasing) filter at the input of the analog-to-digital converter (ADC) at the receiving side, assuming perfect frequency-offset compensation, the received baseband signal, after anti-aliasing filtering, is given by $\widetilde{r}_c(t) = \sum_{k=-\infty}^{+\infty} \sum_{p=0}^{P-1} u_p(k)\, h_c(t - p\,T_c - k\,T) + \widetilde{v}_c(t)$, where $h_c(\tau) \triangleq \psi_c(\tau) \star g_c(\tau) \star \phi_c(\tau)$ is the impulse response of the *composite* channel (encompassing the cascade of the DAC interpolation filter, the physical channel, and the ADC anti-aliasing filter), and $\widetilde{v}_c(t)$ represents the (filtered) disturbance (interference-plus-noise) at the output of the ADC anti-aliasing filter. In the rest of the paper, the following assumptions are considered:

A1) the transmitted symbols $\{s(n)\}_{n \in \mathbb{Z}}$ are modeled as a sequence of zero-mean independent and identically distributed complex *noncircular* random variables, with variance $\sigma_s^2 \triangleq \mathrm{E}[|s(n)|^2] > 0$ and second-order moment $\mathrm{E}[s^2(n)] \neq 0$;

A2) the disturbance $\widetilde{v}_c(t)$ is a zero-mean complex circular wide-sense stationary (WSS) random process, statistically independent of the sequence $\{s(n)\}_{n \in \mathbb{Z}}$, with statistical autocorrelation function $R_{\widetilde{v}\widetilde{v}}(\tau) \triangleq \mathrm{E}[\widetilde{v}_c(t)\, \widetilde{v}_c^*(t - \tau)]$;

A3) the channel impulse response $h_c(\tau)$ spans $L \leq L_{\text{cp}}$ sampling periods, i.e., $h_c(\tau) \equiv 0$ for $\tau \notin [0, L\,T_c]$; hence, the resulting discrete time channel $h(m) \triangleq h_c(mT_c)$ is a causal FIR filter of order $L \leq L_{\text{cp}}$, i.e., $h(m) \equiv 0$ for $m \notin \{0, 1, \ldots, L\}$, with $h(0), h(L) \neq 0$.

Assumption A1 is surely verified by real modulation schemes such as m-ASK or BPSK, for which $\mathrm{E}[s^2(n)] = \mathrm{E}[|s(n)|^2] = \sigma_s^2 > 0$, whereas m-PSK ($m > 2$) and QAM constellations, commonly employed in OFDM systems, exhibit $\mathrm{E}[s^2(n)] \equiv 0$ and, thus, do not satisfy A1. Interestingly, however, Assumption A1 is satisfied also by *staggered* or *offset* variants of the latter modulation schemes, such as OQPSK and OQAM (see Section IV for a discussion), which are employed in pulse-shaping multicarrier systems [33] for their robustness to carrier frequency offset.

Let us assume, without loss of generality, that the nth symbol vector $\boldsymbol{s}(n)$ must be estimated. To this aim, the received signal $\widetilde{r}_c(t)$ is sampled, with rate $1/T_c$, at time instants $t_{n,\ell} \triangleq n\,T + \ell\,T_c$, with $\ell \in \{0, 1, \ldots, P-1\}$, yielding thus, under A3, the discrete-time sequence $\widetilde{r}_\ell(n) \triangleq \widetilde{r}_c(t_{n,\ell}) = \sum_{k=n-1}^{n} \sum_{p=0}^{P-1} u_p(k)\, h[(n-k)P + (\ell - p)] + \widetilde{v}_\ell(n)$, for $\ell \in \{0, 1, \ldots, P-1\}$, where we set $h(m) \triangleq h_c(m\,T_c)$ and $\widetilde{v}_\ell(n) \triangleq \widetilde{v}_c(t_{n,\ell})$. By gathering the samples of the sequence $\{\widetilde{r}_\ell(n)\}_{\ell=0}^{P-1}$ into the column vector $\widetilde{\boldsymbol{r}}(n) \triangleq [\widetilde{r}_0(n), \widetilde{r}_1(n), \ldots, \widetilde{r}_{P-1}(n)]^T \in \mathbb{C}^P$ and accounting for (1), we obtain the compact vector model for the received signal (see also [29], [30], [36]):

$$\widetilde{\boldsymbol{r}}(n) = \widetilde{\boldsymbol{H}}_0\, \boldsymbol{T}_0\, \boldsymbol{s}(n) + \widetilde{\boldsymbol{H}}_1\, \boldsymbol{T}_0\, \boldsymbol{s}(n-1) + \widetilde{\boldsymbol{v}}(n)\,, \quad (2)$$

where $\widetilde{\boldsymbol{v}}(n) \triangleq [\widetilde{v}_0(n), \widetilde{v}_1(n), \ldots, \widetilde{v}_{P-1}(n)]^T$ is the overall disturbance vector, while the channel matrices $\widetilde{\boldsymbol{H}}_0, \widetilde{\boldsymbol{H}}_1 \in \mathbb{C}^{P \times P}$, which are Toeplitz lower- and upper-triangular matrices, respectively, are given by

$$\widetilde{\boldsymbol{H}}_0 \triangleq \begin{bmatrix} h(0) & 0 & 0 & \cdots & 0 \\ \vdots & h(0) & 0 & \cdots & 0 \\ h(L) & \cdots & \ddots & \cdots & \vdots \\ \vdots & \ddots & \cdots & \ddots & 0 \\ 0 & \cdots & h(L) & \cdots & h(0) \end{bmatrix} \quad (3)$$

$$\widetilde{\boldsymbol{H}}_1 \triangleq \begin{bmatrix} 0 & \cdots & h(L) & \cdots & h(1) \\ \vdots & \ddots & 0 & \ddots & \vdots \\ 0 & \cdots & \ddots & \cdots & h(L) \\ \vdots & \vdots & \vdots & \ddots & \vdots \\ 0 & \cdots & 0 & \cdots & 0 \end{bmatrix}. \quad (4)$$

III. LINEAR ZF RECEIVERS

A linear receiver is a bank of M linear FIR filters $y_m(n) = \widetilde{\boldsymbol{g}}_m^H\, \widetilde{\boldsymbol{r}}(n)$, $m \in \{0, 1, \ldots, M-1\}$, where $\widetilde{\boldsymbol{g}}_m \in \mathbb{C}^P$ is the mth equalizer weight vector, aimed at recovering the mth symbol $s_m(n)$ belonging to the nth block $\boldsymbol{s}(n)$. The bank of equalizers can be compactly expressed as

$$\boldsymbol{y}(n) = \widetilde{\boldsymbol{G}}\, \widetilde{\boldsymbol{r}}(n)\,, \quad (5)$$

where $\boldsymbol{y}(n) \triangleq [y_0(n), y_1(n), \ldots, y_{M-1}(n)]^T \in \mathbb{C}^M$ and $\widetilde{\boldsymbol{G}} \triangleq [\widetilde{\boldsymbol{g}}_0, \widetilde{\boldsymbol{g}}_1, \ldots, \widetilde{\boldsymbol{g}}_{M-1}]^H \in \mathbb{C}^{M \times P}$. By substituting (2) into (5) and rearranging terms, the equalizer output can be expressed as

$$\boldsymbol{y}(n) = \boldsymbol{s}(n) + \underbrace{(\widetilde{\boldsymbol{G}}\, \widetilde{\boldsymbol{H}}_0\, \boldsymbol{T}_0 - \mathbf{I}_M)\, \boldsymbol{s}(n)}_{\text{(a)}} + \underbrace{\widetilde{\boldsymbol{G}}\, \widetilde{\boldsymbol{H}}_1\, \boldsymbol{T}_0\, \boldsymbol{s}(n-1)}_{\text{(b)}} + \underbrace{\widetilde{\boldsymbol{G}}\, \widetilde{\boldsymbol{v}}(n)}_{\text{(c)}}\,. \quad (6)$$

In (6) we distinguish *three* potential sources of degradation for the detection of the information signal $\boldsymbol{s}(n)$: (a) the intercarrier interference (ICI), due to the fact that $\widetilde{\boldsymbol{G}}\widetilde{\boldsymbol{H}}_0\,\boldsymbol{T}_0$ is not equal to the identity matrix $\mathbf{I}_M$; (b) the interblock interference (IBI), caused by the symbol $\boldsymbol{s}(n-1)$; (c) the disturbance $\widetilde{\boldsymbol{v}}(n)$, which can account for structured (as, for example, NBI) as well as unstructured (i.e., thermal noise) interference. In the following, any receiver completely suppressing both IBI and ICI is referred to as a *zero-forcing* (ZF) receiver.

To achieve perfect IBI suppression for any value of $\boldsymbol{s}(n-1)$, we require in (6) that $\widetilde{\boldsymbol{G}}\,\widetilde{\boldsymbol{H}}_1\,\boldsymbol{T}_0 = \mathbf{O}_{M\times M}$. Since $\boldsymbol{T}_0$ is full-column rank, a straightforward generalization to the case $L \leq L_{\text{cp}}$ of the results in [29, Eq.(23)] (derived for $L = L_{\text{cp}}$) shows that the general form of an IBI-free receiver is

$$\widetilde{\boldsymbol{G}} = [\mathbf{O}_{M\times L}, \boldsymbol{G}\,] \,, \tag{7}$$

where $\boldsymbol{G} \in \mathbb{C}^{M\times N}$, with $N \triangleq P - L$, is an arbitrary matrix, whose complex entries represent the MN remaining degrees of freedom, which can be exploited to satisfy some additional optimization criterion (e.g., the ICI-free condition). By substituting (7) into (5), we observe that an IBI-free equalizer discards in practice the first L elements of $\widetilde{\boldsymbol{r}}(n)$ which, by virtue of the particular structure (4) of $\widetilde{\boldsymbol{H}}_1$, contain the IBI contribution $\boldsymbol{s}(n-1)$. However, note that implementation of (7) requires *exact* knowledge of the channel order L. In practice, the exact value of L is seldom known in advance, instead an upper bound on L is available, on the basis of which the CP length is set at the transmitter side so as to satisfy $L_{\text{cp}} \geq L$. Therefore, renouncing to some degrees of freedom, it is possible to consider an IBI-free *suboptimal* solution, obtained by discarding at the receiver side the *entire* CP. In this case, equation (7) reduces to $\widetilde{\boldsymbol{G}} = [\mathbf{O}_{M\times L_{\text{cp}}}, \boldsymbol{G}\,]$, with $\boldsymbol{G} \in \mathbb{C}^{M\times M}$, and the number of degrees of freedom reduces to M^2. Such a receiver can also be written in the form $\widetilde{\boldsymbol{G}} = \boldsymbol{G}\,\boldsymbol{R}_{\text{cp}}$, where $\boldsymbol{R}_{\text{cp}} \triangleq (\mathbf{O}_{M\times L_{\text{cp}}}, \mathbf{I}_M) \in \mathbb{R}^{M\times P}$ is the CP removal matrix. The resulting IBI-free equalizer has a *two-stage* structure: the first stage $\boldsymbol{R}_{\text{cp}}$ suppresses IBI, by removing the first L_{cp} samples (corresponding to the CP) from the received vector, whereas the second one performs a linear processing of the remaining M samples by means of the matrix $\boldsymbol{G}$. Indeed, one has

$$\boldsymbol{y}(n) = \boldsymbol{G}\,\boldsymbol{R}_{\text{cp}}\,\widetilde{\boldsymbol{r}}(n) = \boldsymbol{G}\,\boldsymbol{r}(n) \,, \tag{8}$$

where the output of the first stage can be written in the form

$$\boldsymbol{r}(n) \triangleq \boldsymbol{R}_{\text{cp}}\,\widetilde{\boldsymbol{r}}(n) = \boldsymbol{H}_0\,\boldsymbol{T}_0\,\boldsymbol{s}(n) + \boldsymbol{v}(n) \,, \tag{9}$$

whereas $\boldsymbol{v}(n) \triangleq \boldsymbol{R}_{\text{cp}}\widetilde{\boldsymbol{v}}(n)$ is the vector formed from the last M elements of $\widetilde{\boldsymbol{v}}(n)$, and the channel Toeplitz matrix $\boldsymbol{H}_0 \triangleq \boldsymbol{R}_{\text{cp}}\widetilde{\boldsymbol{H}}_0 \in \mathbb{C}^{M\times P}$ contains the last M rows of $\widetilde{\boldsymbol{H}}_0$.

Since the first stage of an IBI-free receiver is *fixed*, we focus on the synthesis of the second stage, i.e., the determination of matrix $\boldsymbol{G}$. By substituting (9) into (8), one has $\boldsymbol{y}(n) = \boldsymbol{G}\,\boldsymbol{r}(n) = \boldsymbol{G}\,\boldsymbol{H}_0\,\boldsymbol{T}_0\,\boldsymbol{s}(n) + \boldsymbol{G}\,\boldsymbol{v}(n)$. Let us impose the ICI-free condition into the previous equation, corresponding to perfect ICI cancellation, i.e.,

$$\boldsymbol{G}\,\underbrace{\boldsymbol{H}_0\,\boldsymbol{T}_0}_{\boldsymbol{F}_0\in\mathbb{C}^{M\times M}} = \mathbf{I}_M \,, \tag{10}$$

which must be regarded as a linear matrix equation in the unknown $\boldsymbol{G}$. Since both $\boldsymbol{G}$ and $\boldsymbol{F}_0$ belong to $\mathbb{C}^{M\times M}$, equation (10) admits a solution if and only if (iff) $\boldsymbol{F}_0$ is nonsingular, which is a condition discussed in the following Lemma (see, e.g., [36] for a proof).

Lemma 1 (Linear ZF equalizability condition): The matrix $\boldsymbol{F}_0$ in (10) is nonsingular iff the M-point DFT $H(k)$ of the discrete-time channel $\{h(n)\}_{n=0}^{L}$ has no zero, i.e., $H(k) \neq 0$, $\forall k \in \{0, 1, \ldots, M-1\}$.

Lemma 1 assures the *existence* and *uniqueness* of linear ZF receivers. Indeed, under Lemma 1, the unique solution of (10) is the inverse of $\boldsymbol{F}_0$. Since $\boldsymbol{F}_0 = \boldsymbol{W}_{\text{IDFT}}\boldsymbol{\mathcal{H}}$, where $\boldsymbol{\mathcal{H}} \triangleq \text{diag}[H(0), H(1), \ldots, H(M-1)] \in \mathbb{C}^{M\times M}$ (see [36]), it turns out that $\boldsymbol{G}_{\text{zf}} = \boldsymbol{F}_0^{-1} = \boldsymbol{\mathcal{H}}^{-1}\boldsymbol{W}_{\text{DFT}}$ and, hence, the linear ZF receiver (including CP removal) is given by $\widetilde{\boldsymbol{G}}_{\text{zf}} = \boldsymbol{G}_{\text{zf}}\boldsymbol{R}_{\text{cp}} = \boldsymbol{\mathcal{H}}^{-1}\boldsymbol{W}_{\text{DFT}}\boldsymbol{R}_{\text{cp}}$, i.e., it boils down to the conventional OFDM receiver, which performs in the given order the following operations on the received signal $\widetilde{\boldsymbol{r}}(n)$: CP removal, DFT, and frequency-domain equalization (FEQ). It is worthwhile to note that the ICI-free constraint (10) *consumes* all the M^2 degrees of freedom, thus the resulting solution is unique, does not depend on the received data, and hence it is not possible to further optimize the receiver, namely, to counteract the effects of noise-plus-interference [term (c) in (6)]. Finally, to overcome the limited NBI suppression capability of the linear ZF receiver, one can renounce to the ICI-free constraint (10) and synthesize instead the IBI-free minimum-mean square-error (MMSE) receiver starting from (8) and (9). More precisely, the filtering matrix $\boldsymbol{G}$ is chosen such as to minimize the MSE $\triangleq \text{E}[\|\boldsymbol{y}(n) - \boldsymbol{s}(n)\|^2]$, whose solution is $\boldsymbol{G}_{\text{mmse}} = \boldsymbol{F}_0^H\boldsymbol{R}_{\boldsymbol{rr}}^{-1}$. However, simulation results reported in Section VI show that also the MMSE receiver is unable to assure satisfactory NBI suppression in many scenarios.

IV. Widely-linear ZF receivers

When $\boldsymbol{s}(n)$ is a noncircular vector process [24], the number of degrees of freedom can be increased by linearly processing *both* $\widetilde{\boldsymbol{r}}(n)$ and $\widetilde{\boldsymbol{r}}^*(n)$, i.e.,

$$\boldsymbol{y}(n) = \widetilde{\boldsymbol{G}}_1\,\widetilde{\boldsymbol{r}}(n) + \widetilde{\boldsymbol{G}}_2\,\widetilde{\boldsymbol{r}}^*(n) \,. \tag{11}$$

Receivers like (11) are usually referred in the literature to as *linear conjugate-linear* [2], [3] or *widely-linear* (WL) [24]. The class of linear receivers (5) can be trivially regarded as a *subclass* of WL ones, obtained setting $\widetilde{\boldsymbol{G}}_1 \triangleq \widetilde{\boldsymbol{G}}$ and $\widetilde{\boldsymbol{G}}_2 \triangleq \mathbf{O}_{M\times P}$ in (11). Thus, a linear receiver *cannot* exhibit better performance (according to any criterion) than a WL one. As a matter of fact, we show in the following that WL processing might assure substantial advantages not only in terms of equalization performance, but also in terms of improved blind channel identification capabilities (see Section V).

A. IBI elimination in WL receivers

By substituting (2) into (11), the output of a WL equalizer can be expressed as

$$\boldsymbol{y}(n) = \boldsymbol{s}(n) + \underbrace{(\widetilde{\boldsymbol{G}}_1 \widetilde{\boldsymbol{H}}_0 \boldsymbol{T}_0 - \mathbf{I}_M)\, \boldsymbol{s}(n) + \widetilde{\boldsymbol{G}}_2 \widetilde{\boldsymbol{H}}_0^* \boldsymbol{T}_0^* \boldsymbol{s}^*(n)}_{\text{(a)}} + \underbrace{\widetilde{\boldsymbol{G}}_1 \widetilde{\boldsymbol{H}}_1 \boldsymbol{T}_0 \boldsymbol{s}(n-1) + \widetilde{\boldsymbol{G}}_2 \widetilde{\boldsymbol{H}}_1^* \boldsymbol{T}_0^* \boldsymbol{s}^*(n-1)}_{\text{(b)}} + \underbrace{\widetilde{\boldsymbol{G}}_1 \widetilde{\boldsymbol{v}}(n) + \widetilde{\boldsymbol{G}}_2 \widetilde{\boldsymbol{v}}^*(n)}_{\text{(c)}}, \quad (12)$$

where the terms denoted with (a), (b), (c) represent, as in the linear case (6), the ICI, the IBI, and the disturbance contributions. In order to avoid IBI, we require that $\widetilde{\boldsymbol{G}}_1$ and $\widetilde{\boldsymbol{G}}_2$ satisfy

$$\widetilde{\boldsymbol{G}}_1 \widetilde{\boldsymbol{H}}_1 \boldsymbol{T}_0 = \mathbf{O}_{M\times M} \quad \text{and} \quad \widetilde{\boldsymbol{G}}_2 \widetilde{\boldsymbol{H}}_1^* \boldsymbol{T}_0^* = \mathbf{O}_{M\times M}\,. \quad (13)$$

Each equation is similar in form to the IBI-free condition for the linear case, moreover the two equations in $\widetilde{\boldsymbol{G}}_1$ and $\widetilde{\boldsymbol{G}}_2$ are decoupled. Hence, reasoning as in the linear case, we maintain that the WL IBI-free solution, under the assumption that the entire CP is removed at the receiving side, is given by

$$\widetilde{\boldsymbol{G}}_1 = (\mathbf{O}_{M\times L_{\text{cp}}}, \boldsymbol{G}_1) \quad \text{and} \quad \widetilde{\boldsymbol{G}}_2 = (\mathbf{O}_{M\times L_{\text{cp}}}, \boldsymbol{G}_2)\,, \quad (14)$$

where $\boldsymbol{G}_1, \boldsymbol{G}_2 \in \mathbb{C}^{M\times M}$ contain the $2M^2$ remaining degrees of freedom. Equivalently, we set $\widetilde{\boldsymbol{G}}_1 = \boldsymbol{G}_1 \boldsymbol{R}_{\text{cp}}$ and $\widetilde{\boldsymbol{G}}_2 = \boldsymbol{G}_2 \boldsymbol{R}_{\text{cp}}$ in (12), obtaining

$$\boldsymbol{y}(n) = \boldsymbol{G}_1 \boldsymbol{H}_0 \boldsymbol{T}_0 \boldsymbol{s}(n) + \boldsymbol{G}_2 \boldsymbol{H}_0^* \boldsymbol{T}_0^* \boldsymbol{s}^*(n) + \boldsymbol{G}_1 \boldsymbol{v}(n) + \boldsymbol{G}_2 \boldsymbol{v}^*(n)\,. \quad (15)$$

B. ICI elimination in WL receivers

Since we are interested in recovering $\boldsymbol{s}(n)$, we could treat $\boldsymbol{s}(n)$ as useful signal and $\boldsymbol{s}^*(n)$ as disturbance: in this case, the ICI-free condition would be written as

$$\boldsymbol{G}_1 \boldsymbol{H}_0 \boldsymbol{T}_0 = \mathbf{I}_M \quad \text{and} \quad \boldsymbol{G}_2 \boldsymbol{H}_0^* \boldsymbol{T}_0^* = \mathbf{O}_{M\times M}\,. \quad (16)$$

Observe that the first condition in (16), with $\boldsymbol{G}_1$ *in lieu* of $\boldsymbol{G}$, is the same as (10) for the linear case, a solution exists iff Lemma 1 holds, i.e., iff $\text{rank}(\boldsymbol{H}_0 \boldsymbol{T}_0) = M$; in this case, one has $\boldsymbol{G}_1 = \boldsymbol{\mathcal{H}}^{-1} \boldsymbol{W}_{\text{DFT}}$. Note that $\text{rank}(\boldsymbol{H}_0^* \boldsymbol{T}_0^*) = \text{rank}(\boldsymbol{H}_0 \boldsymbol{T}_0)$, hence if Lemma 1 holds, the second equation in (16) admits only the trivial solution $\boldsymbol{G}_2 = \mathbf{O}_{M\times M}$. Therefore, the ICI-free conditions are verified iff Lemma 1 holds, and the resulting WL-ZF receiver is uniquely given by

$$\boldsymbol{G}_1 = \boldsymbol{G}_{\text{zf}} = \boldsymbol{\mathcal{H}}^{-1} \boldsymbol{W}_{\text{DFT}} \quad \text{and} \quad \boldsymbol{G}_2 = \mathbf{O}_{M\times M}\,. \quad (17)$$

Since $\boldsymbol{G}_2 = \mathbf{O}_{M\times M}$, this WL-ZF receiver degenerates into a linear receiver; more precisely, it degenerates into the *unique* linear ZF receiver represented by the OFDM conventional receiver. In conclusion, if we treat $\boldsymbol{s}^*(n)$ as disturbance, i.e., we synthesize the WL-ZF receiver as if $\boldsymbol{s}(n)$ and $\boldsymbol{s}^*(n)$ were *functionally* independent, then WL processing does not assure any advantage over linear one. On the other hand, in the framework of minimum mean-square error (MMSE) optimization, it is well known [24] that WL processing is advantageous when one exploits the linear *statistical* dependence between $\boldsymbol{s}(n)$ and $\boldsymbol{s}^*(n)$. In our case, however, since we want to enforce a *deterministic* ICI-free constraint on $\boldsymbol{s}(n)$, we must turn this linear statistical dependence into a deterministic linear relationship between $\boldsymbol{s}(n)$ and $\boldsymbol{s}^*(n)$. To this aim, we first observe that, for the mth subcarrier, $\text{E}[s_m^2(n)]$ can be regarded as a scalar product between $s_m(n)$ and $s_m^*(n)$. Hence, by the Schwartz inequality, its magnitude is maximized when $s_m^*(n) = \phi_m(n)\, s_m(n)$, where $\phi_m(n)$ is an arbitrary deterministic complex sequence.[1] By averaging the squared magnitudes of both sides of the previous relation, we obtain $\text{E}[|s_m(n)|^2] = |\phi_m(n)|^2 \text{E}[|s_m(n)|^2]$, from which $|\phi_m(n)| = 1$ necessarily. Since $s_m(n)$ is a digitally-modulated sequence, it is not restrictive to focus attention to the case where $\phi_m(n) = e^{j2\pi\beta n}$, with $\beta \in [0, 1)$, i.e.,

$$s_m^*(n) = e^{j2\pi\beta n}\, s_m(n) \qquad \forall n \in \mathbb{Z}\,. \quad (18)$$

A sequence $s_m(n)$ satisfying (18) is surely non circular, since $|\text{E}[s_m^2(n)]| = \sigma_s^2 > 0$; thus, property (18) is *stronger* than simple noncircularity, and hence can be denominated *strong noncircularity*. Signals exhibiting such a property are sometimes referred in the literature to as *conjugate symmetric* [31] and are widely used in telecommunications, radar, and sonar. They include all memoryless real modulation formats (BPSK, m-ASK), differential schemes (DBPSK), offset schemes (OQPSK, OQAM), and even (in an approximate sense) modulations with memory (binary CPM, MSK, GMSK). For example, real modulation schemes fulfill (18) with $\beta = 0$, i.e., $s_m^*(n) = s_m(n)$, whereas for complex modulation schemes, such as OQPSK, OQAM, and MSK, relation (18) is satisfied [6], [11] if $\beta = 1/2$, i.e., $s_m^*(n) = (-1)^n s_m(n)$. On the contrary, for circular modulation schemes such as QPSK, QAM, or PSK, the condition $\text{E}[s_m^2(n)] \equiv 0$ can be interpreted as *orthogonality* between $s_m(n)$ and $s_m^*(n)$, which means that $s_m^*(n)$ cannot be obtained from $s_m(n)$ by a simple linear relation. In other words, since $s_m^*(n)$ is orthogonal to $s_m(n)$, it acts exactly as a disturbance with respect to $s_m(n)$, and thus the synthesis of the WL-ZF receiver must be carried out as described in (16), leading trivially to the conventional ZF solution (17).

Thus, in the following we assume, in addition to A1, that $s_m(n)$ is strongly noncircular, i.e., it satisfies (18), which entails a linear deterministic relationship between $\boldsymbol{s}(n)$ and $\boldsymbol{s}^*(n)$, of the form

$$\boldsymbol{s}^*(n) = e^{j2\pi\beta n}\, \boldsymbol{s}(n), \qquad \forall n \in \mathbb{Z}\,. \quad (19)$$

Direct substitution of (19) in (15) would yield at the equalized output $\boldsymbol{y}(n) = \boldsymbol{G}_1 \boldsymbol{H}_0 \boldsymbol{T}_0 \boldsymbol{s}(n) + \boldsymbol{G}_2 \boldsymbol{H}_0^* \boldsymbol{T}_0^* e^{j2\pi\beta n} \boldsymbol{s}(n) + \boldsymbol{G}_1 \boldsymbol{v}(n) + \boldsymbol{G}_2 \boldsymbol{v}^*(n)$, which complicates matters due to the presence of the complex exponential $e^{j2\pi\beta n}$. To avoid this, we perform "derotation" of $\boldsymbol{r}^*(n)$ before evaluating $\boldsymbol{y}(n)$ and thus we define the following *augmented* model for the received

[1] Although to assure that the magnitude of the scalar product reaches its maximum it is sufficient that $s_m^*(n) = \phi_m(n)\, s_m(n)$ holds in the mean-square sense, i.e., $\text{E}[|s_m^*(n) - \phi_m(n)\, s_m(n)|^2] = 0$, in the following we assume that the equality holds *everywhere*, i.e., for any realization of the random process $s_m(n)$.

signal:

$$\boldsymbol{z}(n) \triangleq \begin{bmatrix} \boldsymbol{r}(n) \\ \boldsymbol{r}^*(n)\, e^{-j2\pi\beta n} \end{bmatrix} = \underbrace{\begin{bmatrix} \boldsymbol{H}_0\, \boldsymbol{T}_0 \\ \boldsymbol{H}_0^*\, \boldsymbol{T}_0^* \end{bmatrix}}_{\boldsymbol{\mathcal{F}}_0 \in \mathbb{C}^{2M\times M}} \boldsymbol{s}(n) + \underbrace{\begin{bmatrix} \boldsymbol{v}(n) \\ \boldsymbol{v}^*(n)\, e^{-j2\pi\beta n} \end{bmatrix}}_{\boldsymbol{d}(n)\in\mathbb{C}^{2M}} = \boldsymbol{\mathcal{F}}_0\, \boldsymbol{s}(n) + \boldsymbol{d}(n)\,. \quad (20)$$

Equation (15) after derotation can hence be written as

$$\boldsymbol{y}(n) = \boldsymbol{\mathcal{G}}\, \boldsymbol{z}(n) = \boldsymbol{\mathcal{G}}\, \boldsymbol{\mathcal{F}}_0\, \boldsymbol{s}(n) + \boldsymbol{\mathcal{G}}\, \boldsymbol{d}(n)\,, \quad (21)$$

where $\boldsymbol{\mathcal{G}} \triangleq (\boldsymbol{G}_1, \boldsymbol{G}_2) \in \mathbb{C}^{M\times 2M}$. Noting that $\boldsymbol{H}_0 \boldsymbol{T}_0 = \boldsymbol{F}_0 = \boldsymbol{W}_{\text{IDFT}} \boldsymbol{\mathcal{H}}$, matrix $\boldsymbol{\mathcal{F}}_0$ can be rewritten as

$$\boldsymbol{\mathcal{F}}_0 = \begin{bmatrix} \boldsymbol{F}_0 \\ \boldsymbol{F}_0^* \end{bmatrix} = \begin{bmatrix} \boldsymbol{W}_{\text{IDFT}} \boldsymbol{\mathcal{H}} \\ \boldsymbol{W}_{\text{IDFT}}^* \boldsymbol{\mathcal{H}}^* \end{bmatrix} = \underbrace{\begin{bmatrix} \boldsymbol{W}_{\text{IDFT}} & \mathbf{O}_{M\times M} \\ \mathbf{O}_{M\times M} & \boldsymbol{W}_{\text{IDFT}}^* \end{bmatrix}}_{\boldsymbol{W}} \underbrace{\begin{bmatrix} \boldsymbol{\mathcal{H}} \\ \boldsymbol{\mathcal{H}}^* \end{bmatrix}}_{\boldsymbol{B}}, \quad (22)$$

where, since $\boldsymbol{W}_{\text{DFT}}$ is nonsingular, the block-diagonal matrix $\boldsymbol{W} \in \mathbb{C}^{2M\times 2M}$ is nonsingular. According to (21), the ICI-free condition can be restated[2] as

$$\boldsymbol{\mathcal{G}}\, \boldsymbol{\mathcal{F}}_0 = \mathbf{I}_M\,. \quad (23)$$

Equation (23) in the unknown matrix $\boldsymbol{\mathcal{G}}$ admits solutions iff $\text{rank}(\boldsymbol{\mathcal{F}}_0) = M$, i.e., matrix $\boldsymbol{\mathcal{F}}_0$ must be full-column rank. The following Lemma, similar in spirit to Lemma 1, holds.

Lemma 2 (WL-ZF equalizability condition): The matrix $\boldsymbol{\mathcal{F}}_0$ in (20) is full-column rank iff the M-point DFT $H(k)$ of the discrete-time channel $\{h(n)\}_{n=0}^{L}$ has no zero, i.e., $H(k) \neq 0$, $\forall k \in \{0, 1, \ldots, M-1\}$.

Proof: See Appendix I. ■

Let us note that, notwithstanding their different structures, the condition required for the existence of WL-ZF receivers expressed by Lemma 2 is *exactly* the same as that expressed by Lemma 1 for the linear case. In this regard, WL processing does not extend the class of channels that can be perfectly equalized beyond that of the linear case. However, the advantage of WL processing is that, since $\boldsymbol{\mathcal{F}}_0$ is tall by construction, the solution $\boldsymbol{\mathcal{G}}$ of equation (23) is *not* unique and, thus, the additional degrees of freedom can be utilized to reduce the noise-plus-NBI contribution, according to a given criterion. Indeed, assuming Lemma 2 to hold, the linear solution given by (17) is a *particular* solution of (23). The general solution of (23), instead, can be written [22] as

$$\boldsymbol{\mathcal{G}} = \underbrace{\boldsymbol{\mathcal{F}}_0^\dagger}_{\boldsymbol{\mathcal{G}}^{(\text{f})}\in\mathbb{C}^{M\times 2M}} + \underbrace{\boldsymbol{\mathcal{Y}}\, [\mathbf{I}_{2M} - \boldsymbol{\mathcal{F}}_0 \boldsymbol{\mathcal{F}}_0^\dagger]}_{\boldsymbol{\mathcal{G}}^{(\text{a})}\in\mathbb{C}^{M\times 2M}}, \quad (24)$$

where $\boldsymbol{\mathcal{Y}} \in \mathbb{C}^{M\times 2M}$ is an arbitrary complex matrix. The WL-ZF receiver $\boldsymbol{\mathcal{G}}$ can be regarded as the sum of a *fixed* $\boldsymbol{\mathcal{G}}^{(\text{f})}$, representing a particular solution of (23), and a *free* or *adaptive* (i.e., depending on $\boldsymbol{\mathcal{Y}}$) $\boldsymbol{\mathcal{G}}^{(\text{a})}$, which represents the *general* solution of the homogeneous equation associated to (23). Moreover, the summands $\boldsymbol{\mathcal{G}}^{(\text{f})}$ and $\boldsymbol{\mathcal{G}}^{(\text{a})}$ are orthogonal, for any choice of $\boldsymbol{\mathcal{Y}}$, namely $\boldsymbol{\mathcal{G}}^{(\text{f})}\, [\boldsymbol{\mathcal{G}}^{(\text{a})}]^H = \mathbf{O}_{M\times M}$. In this sense, such a canonical decomposition (24) is the natural generalization to the matrix case of the so-called *generalized sidelobe canceler* (GSC) decomposition [13], which is well known in the array processing context.

Since each column of $[\boldsymbol{\mathcal{G}}^{(\text{a})}]^H$ belongs to $\text{range}^\perp(\boldsymbol{\mathcal{F}}_0)$, which has dimensionality M, it is possible to parameterize $\boldsymbol{\mathcal{G}}^{(\text{a})}$ by only M^2 free complex numbers. Indeed, by taking into account the structure of $\boldsymbol{\mathcal{F}}_0$ and applying straightforward matrix algebra, both $\boldsymbol{\mathcal{G}}^{(\text{f})}$ and $\boldsymbol{\mathcal{G}}^{(\text{a})}$ can be explicitly computed as

$$\boldsymbol{\mathcal{G}}^{(\text{f})} = \frac{1}{2} \left[\boldsymbol{\mathcal{H}}^{-1} \boldsymbol{W}_{\text{DFT}}\,,\ (\boldsymbol{\mathcal{H}}^{-1})^* \boldsymbol{W}_{\text{DFT}}^* \right]\,, \quad (25)$$

$$\boldsymbol{\mathcal{G}}^{(\text{a})} = \boldsymbol{Y}\, \underbrace{\frac{1}{\sqrt{2}} \left[\mathbf{I}_M\,,\ -\boldsymbol{W}_{\text{DFT}}^* \boldsymbol{\mathcal{H}} (\boldsymbol{\mathcal{H}}^{-1})^* \boldsymbol{W}_{\text{DFT}}^* \right]}_{\boldsymbol{\mathcal{P}}\in\mathbb{C}^{M\times 2M}}, \quad (26)$$

where the entries $\boldsymbol{Y} \in \mathbb{C}^{M\times M}$ represent the *effective* M^2 degrees of freedom of the problem, and the columns of $\boldsymbol{\mathcal{P}}^H$ constitute an orthonormal basis for $\text{range}^\perp(\boldsymbol{\mathcal{F}}_0)$, i.e., $\boldsymbol{\mathcal{P}}\, \boldsymbol{\mathcal{F}}_0 = \mathbf{O}_{M\times M}$ and $\boldsymbol{\mathcal{P}} \boldsymbol{\mathcal{P}}^H = \mathbf{I}_M$.

C. MV and MOE interference mitigation

We exploit in this Section the remaining M^2 degrees of freedom, contained in matrix $\boldsymbol{Y}$, to mitigate the effects of the disturbance, by minimizing its contribution to the variance of the output equalizer. Such a task can be simplified if we exploit again the GSC decomposition (24). Indeed, by substituting (24) in (21), and accounting for (26) and (23), one has

$$\begin{aligned} \boldsymbol{y}(n) = \boldsymbol{\mathcal{G}}\, \boldsymbol{z}(n) &= \boldsymbol{\mathcal{G}}\, \boldsymbol{\mathcal{F}}_0\, \boldsymbol{s}(n) + \boldsymbol{\mathcal{G}}\, \boldsymbol{d}(n) \\ &= \boldsymbol{s}(n) + (\boldsymbol{\mathcal{G}}^{(\text{f})} + \boldsymbol{\mathcal{G}}^{(\text{a})})\, \boldsymbol{d}(n) \\ &= \boldsymbol{s}(n) + (\boldsymbol{\mathcal{G}}^{(\text{f})} + \boldsymbol{Y}\, \boldsymbol{\mathcal{P}})\, \boldsymbol{d}(n)\,. \end{aligned} \quad (27)$$

Thus, interference mitigation can be performed by solving one of the following *unconstrained* quadratic optimization problems:

(a) *WL-ZF minimum-variance (MV)* optimization problem: minimize $\text{E}[\|(\boldsymbol{\mathcal{G}}^{(\text{f})} + \boldsymbol{Y}\boldsymbol{\mathcal{P}})\, \boldsymbol{d}(n)\|^2]$ w.r.t $\boldsymbol{Y} \in \mathbb{C}^{M\times M}$, whose solution is given [8] by

$$\boldsymbol{Y}_{\text{MV}} = -\boldsymbol{\mathcal{G}}^{(\text{f})} \boldsymbol{R}_{\boldsymbol{dd}} \boldsymbol{\mathcal{P}}^H \left(\boldsymbol{\mathcal{P}}\, \boldsymbol{R}_{\boldsymbol{dd}} \boldsymbol{\mathcal{P}}^H \right)^{-1}\,, \quad (28)$$

where, accounting for assumption A2 (circularity of the disturbance), the autocorrelation matrix $\boldsymbol{R}_{\boldsymbol{dd}} \triangleq \text{E}[\, \boldsymbol{d}(n)\, \boldsymbol{d}^H(n)] \in \mathbb{C}^{2M\times 2M}$ does not depend on n.

(b) *WL-ZF minimum-output energy (MOE)* optimization problem: minimize $\text{E}[\|(\boldsymbol{\mathcal{G}}^{(\text{f})} + \boldsymbol{Y}\boldsymbol{\mathcal{P}})\, \boldsymbol{z}(n)\|^2]$ w.r.t $\boldsymbol{Y} \in \mathbb{C}^{M\times M}$, whose solution is given [14] by

$$\boldsymbol{Y}_{\text{MOE}} = -\boldsymbol{\mathcal{G}}^{(\text{f})} \boldsymbol{R}_{\boldsymbol{zz}} \boldsymbol{\mathcal{P}}^H \left(\boldsymbol{\mathcal{P}}\, \boldsymbol{R}_{\boldsymbol{zz}} \boldsymbol{\mathcal{P}}^H \right)^{-1}\,, \quad (29)$$

with $\boldsymbol{R}_{\boldsymbol{zz}} \triangleq \text{E}[\, \boldsymbol{z}(n)\, \boldsymbol{z}^H(n)] \in \mathbb{C}^{2M\times 2M}$.

[2] Note that, in principle, strong noncircularity (19) could be exploited also to derive a different IBI-free condition, which is less restrictive than (13), allowing hence to further increase the number of available degrees of freedom. However, in this case, the structure of the IBI-free receiver would become cumbersome and, hence, although suboptimal, we have chosen to exploit the strong noncircularity property only in the ICI-free condition.

It is worthwhile to note that the two problems turn out to be equivalent since, according to (20) and accounting for A1-A2, the autocorrelation matrix $\boldsymbol{R_{zz}}$ can be expressed as

$$\boldsymbol{R_{zz}} = \sigma_s^2\, \boldsymbol{\mathcal{F}}_0\, \boldsymbol{\mathcal{F}}_0^H + \boldsymbol{R_{dd}}\, . \tag{30}$$

Hence, since $\boldsymbol{\mathcal{P}}\, \boldsymbol{\mathcal{F}}_0 = \mathbf{O}_{M\times M}$ [recall that the columns of $\boldsymbol{\mathcal{P}}^H$ belong to range$^{\perp}(\boldsymbol{\mathcal{F}}_0)$], it results that $\boldsymbol{R_{zz}}\, \boldsymbol{\mathcal{P}}^H = \boldsymbol{R_{dd}}\, \boldsymbol{\mathcal{P}}^H$ and thus (28) and (29) coincide.[3] However, the WL-ZF MOE solution (29) is better suited to implementation, since it is expressed in terms of the autocorrelation matrix $\boldsymbol{R_{zz}}$ of the received signal (20) which, unlike $\boldsymbol{R_{dd}}$, can be directly estimated from the received data by batch or adaptive algorithms.

Turning to complexity issues, note that $\boldsymbol{\mathcal{G}}^{(\text{f})}$ is fixed and can be implemented [see (25)], by means of FFT, one-tap equalization, and conjugate operations. The major computational burden arises from evaluation of $\boldsymbol{\mathcal{G}}^{(\text{a})}$ from received data and real-time multiplication of the received vector with $\boldsymbol{\mathcal{G}}^{(\text{a})}$ to obtain the adaptive part of $\boldsymbol{y}(n)$. While the latter is inherently an $O(M^2)$ operation, evaluation of $\boldsymbol{\mathcal{G}}^{(\text{a})}$ from received data requires [see (28) or (29)] one inversion of an $M \times M$ matrix, which is an $O(M^3)$ operation. However, following the lines of [8], one can easily derive RLS-like adaptive solutions for $\boldsymbol{\mathcal{G}}^{(\text{a})}$ exhibiting only a quadratic complexity in M (for each iteration) and hence the overall computational complexity of the proposed algorithm becomes $O(M^2)$, which nevertheless reveals that this kind of processing can be applied only to systems with a moderate number of subcarriers. However, this is not a shortcoming of WL processing itself, but rather of any reception technique (like e.g. [29]) that attempts to improve upon the conventional OFDM receiver.[4]

V. SUBSPACE-BASED BLIND CHANNEL IDENTIFICATION

Implementation of ZF, MMSE and WL-ZF receivers requires channel knowledge (condensed in matrix $\boldsymbol{\mathcal{H}}$) even in the simplest white disturbance case. To avoid the loss of spectral efficiency resulting from the use of training symbols, in this section we propose a subspace-based algorithm for *blind* channel identification, which exploits the (strong) noncircularity property (19) by WL processing the received vector $\boldsymbol{r}(n)$ (after CP removal) given by (9).

Subspace methods rely on an input-output relationship of the form $\boldsymbol{r}(n) = \boldsymbol{\mathcal{T}}\, \boldsymbol{s}(n) + \boldsymbol{v}(n)$, where the *transfer matrix* $\boldsymbol{\mathcal{T}}$ is tall and full-column rank, $\boldsymbol{s}(n)$ is the symbol vector with nonsingular autocorrelation matrix $\boldsymbol{R_{ss}}$, and $\boldsymbol{v}(n)$ is a disturbance with known and nonsingular autocorrelation matrix $\boldsymbol{R_{vv}}$. All the previous hypotheses are satisfied in (9), except for the transfer matrix $\boldsymbol{\mathcal{T}} = \boldsymbol{F}_0 = \boldsymbol{H}_0 \boldsymbol{T}_{\text{cp}}$, which is not tall. To circumvent this problem, in [21] two consecutive OFDM symbols are concatenated before building the autocorrelation matrix. We take here a different approach, by resorting to the *augmented* model (20) for the received signal. In fact, observe that in (20) the role of the transfer matrix $\boldsymbol{\mathcal{T}}$ is played by $\boldsymbol{\mathcal{F}}_0$, which is tall by construction and, moreover, full-column rank under Lemma 2. Since the full-column rank property of $\boldsymbol{\mathcal{F}}_0$ is crucial, in the following derivations, we assume that the condition of Lemma 2 holds hereinafter. Moreover, in this section we also assume that the disturbance $\boldsymbol{v}(n)$ is white, with variance σ_v^2, whereas the generalization to the case of NBI is discussed in Section V-A.

The proposed algorithm relies on the eigenstructure of $\boldsymbol{R_{zz}}$, which can be obtained from (30) by additionally taking into account that the disturbance is white, thus, yielding

$$\boldsymbol{R_{zz}} = \sigma_s^2\, \boldsymbol{\mathcal{F}}_0\, \boldsymbol{\mathcal{F}}_0^H + \sigma_v^2\, \mathbf{I}_{2M}\, . \tag{31}$$

Let $\lambda_0 \geq \lambda_1 \geq \cdots \geq \lambda_{2M-1}$ denote the $2M$ eigenvalues of $\boldsymbol{R_{zz}}$, and let $\boldsymbol{e}_0, \boldsymbol{e}_1, \ldots, \boldsymbol{e}_{2M-1}$ denote the corresponding orthonormal eigenvectors. Since rank$(\boldsymbol{\mathcal{F}}_0) = M$, the signal component $\sigma_s^2\, \boldsymbol{\mathcal{F}}_0\, \boldsymbol{\mathcal{F}}_0^H$ in (31) has rank M, hence $\lambda_i > \sigma_v^2$, $i = 0, 1, \ldots, M-1$, while $\lambda_i = \sigma_v^2$, $i = M, M+1, \ldots, 2M-1$. Accordingly, the eigenvectors can be partitioned as $\boldsymbol{E}_s = [\boldsymbol{e}_0, \boldsymbol{e}_1, \ldots, \boldsymbol{e}_{M-1}] \in \mathbb{C}^{2M\times M}$ and $\boldsymbol{E}_d = [\boldsymbol{e}_M, \boldsymbol{e}_{M+1}, \ldots, \boldsymbol{e}_{2M-1}] \in \mathbb{C}^{2M\times M}$, with the columns of $\boldsymbol{E}_s$ spanning the so-called *signal subspace*, and the columns of $\boldsymbol{E}_d$ spanning its orthogonal complement in $\mathbb{C}^{2M}$, referred to as the *noise subspace*, both of dimensionality M. The signal subspace is spanned also by the columns of $\boldsymbol{\mathcal{F}}_0$, therefore such columns must be orthogonal to the noise subspace, i.e.,

$$\boldsymbol{E}_d^H\, \boldsymbol{\mathcal{F}}_0 = \mathbf{O}_{M\times M}\, . \tag{32}$$

Let us recall the structure of $\boldsymbol{\mathcal{F}}_0$ given by (22), i.e., $\boldsymbol{\mathcal{F}}_0 = \boldsymbol{W}\, \boldsymbol{B}(\boldsymbol{h})$, where the dependence of $\boldsymbol{B}$ on the channel vector $\boldsymbol{h} \triangleq [h(0), h(1), \ldots, h(L)]^T \in \mathbb{C}^{L+1}$ has been made explicit [see (22)]. Since $\boldsymbol{W}$ is nonsingular, rank$(\boldsymbol{\mathcal{F}}_0) =$ rank$[\boldsymbol{B}(\boldsymbol{h})]$ and, hence, Lemma 2 assures that $\boldsymbol{B}(\boldsymbol{h})$ is full-column rank. Thus, the orthogonality condition (32) can be rewritten as

$$\boldsymbol{E}_d^H\, \boldsymbol{W}\, \boldsymbol{B}(\boldsymbol{h}) = \widetilde{\boldsymbol{E}}_d^H\, \boldsymbol{B}(\boldsymbol{h}) = \mathbf{O}_{M\times M}\, , \tag{33}$$

where $\widetilde{\boldsymbol{E}}_d = [\widetilde{\boldsymbol{e}}_M, \widetilde{\boldsymbol{e}}_{M+1}, \ldots, \widetilde{\boldsymbol{e}}_{2M-1}] \triangleq \boldsymbol{W}^H\, \boldsymbol{E}_d \in \mathbb{C}^{2M\times M}$. By exploiting the particular structure of $\boldsymbol{B}(\boldsymbol{h})$, (33) can be easily turned into an overdetermined linear system in the unknown channel coefficients, which allows one to easily perform channel estimation, provided that (33) *uniquely* characterizes the channel. To this end, we provide the following identifiability theorem.

Theorem 1 (WL identifiability conditions): Let us assume that: (i) $\boldsymbol{\mathcal{F}}_0$ is full-column rank, i.e., rank$(\boldsymbol{\mathcal{F}}_0) = M$; (ii) $M \geq 2L+1$; (iii) the channel transfer function $H(z) = \sum_{\ell=0}^{L} h(\ell)\, z^{-\ell}$ has no zeros in pairs of the type z_0 and $1/z_0^*$. Then, the following statements are equivalent:

(1) The vector $\boldsymbol{h}' = [h'(0), h'(1), \ldots, h'(L)]^T \in \mathbb{C}^{L+1}$ is a solution of (33).

(2) $\boldsymbol{h}' = \alpha\, \boldsymbol{h}$, with $\alpha \in \mathbb{R}$, i.e., the channels $h'(n)$ and $h(n)$ differ by a *real* multiplicative factor.

Proof: See Appendix II. ■

Note that condition $M \geq 2L+1$ is less restrictive than its counterpart $M \geq 2L_{\text{cp}}$ adopted by the blind identification technique of [21], and is always satisfied in practical systems, since the CP length L_{cp} is usually not greater than $M/4$ to limit the amount of introduced redundancy. Compared with

[3] It should be noted, moreover, that both MV and MOE optimizations amount to maximizing the signal-to-noise ratio (SNR) at the WL-ZF equalizer output, which is the criterion adopted in [29] for the linear case.

[4] An interesting way to reduce the algorithm complexity when M is large is the extension to this scenario of the *partially-adaptive* schemes (see [35] and references therein), which have proven fruitful in array processing.

other subspace-based blind identification techniques [21], [27], [26], a peculiar feature of the proposed method is that the dimensions of both the signal and noise subspaces turn out to be M *regardless of the channel order* L. Hence, the Theorem continues to hold when the true channel length L is replaced with an upper bound $L_{\text{est}} \geq L$, with $M \geq 2L_{\text{est}}+1$, i.e., an arbitrary vector $\boldsymbol{h}' \in \mathbb{C}^{L_{\text{est}}+1}$, is a solution of (33) iff $\boldsymbol{h}' = \alpha\,[\boldsymbol{h}^T, \mathbf{0}^T_{L_{\text{est}}-L}]^T$, with $\alpha \in \mathbb{R}$. Finally, on the basis of Theorem 1, the proposed procedure cannot estimate channels with zeros of the type z_0 and $1/z_0^*$, i.e., with reciprocal magnitudes and the same phases.[5] However, simulation results (see example 4 in Section VI) show that the performance of the proposed identification algorithm does not excessively degrade when the zeros location is close to the configuration where the channel is not identifiable.

To estimate the channel in practice, let us rewrite (33), with L_{est} instead of L, as $\boldsymbol{B}^H(\boldsymbol{h})\,\widetilde{\boldsymbol{E}}_d = \mathbf{O}_{M\times M}$. Thus, accounting for (22), one has

$$\text{vec}[\boldsymbol{B}^H(\boldsymbol{h})\,\widetilde{\boldsymbol{E}}_d] = \underbrace{\begin{bmatrix} \boldsymbol{E}_0^{(1)} \\ \boldsymbol{E}_1^{(1)} \\ \vdots \\ \boldsymbol{E}_{M-1}^{(1)} \end{bmatrix}}_{\widetilde{\boldsymbol{E}}^{(1)} \in \mathbb{C}^{M^2\times(L_{\text{est}}+1)}} \boldsymbol{h}^* + \underbrace{\begin{bmatrix} \boldsymbol{E}_0^{(2)} \\ \boldsymbol{E}_1^{(2)} \\ \vdots \\ \boldsymbol{E}_{M-1}^{(2)} \end{bmatrix}}_{\widetilde{\boldsymbol{E}}^{(2)} \in \mathbb{C}^{M^2\times(L_{\text{est}}+1)}} \boldsymbol{h} = \widetilde{\boldsymbol{E}}^{(1)}\boldsymbol{h}^* + \widetilde{\boldsymbol{E}}^{(2)}\boldsymbol{h} \quad (34)$$

where, for $m = 0, 1, \ldots, M-1$, the matrices $\boldsymbol{E}_m^{(1)} \in \mathbb{C}^{M\times(L_{\text{est}}+1)}$ and $\boldsymbol{E}_m^{(2)} \in \mathbb{C}^{M\times(L_{\text{est}}+1)}$ are given by $\{\boldsymbol{E}_m^{(1)}\}_{kn} \triangleq \{e^{+j\frac{2\pi}{M}kn}\,\widetilde{e}_{k,m}\}$ and $\{\boldsymbol{E}_m^{(2)}\}_{kn} \triangleq \{e^{-j\frac{2\pi}{M}kn}\,\widetilde{e}_{k+M,m}\}$, for $k = 0, 1, \ldots, M-1$ and $n = 0, 1, \ldots, L_{\text{est}}$, with $\widetilde{e}_{k,m} \triangleq \{\widetilde{\boldsymbol{E}}_d\}_{km}$. By writing $\boldsymbol{h} = \boldsymbol{h}_R + j\boldsymbol{h}_I$, (34) can be restated as

$$\text{vec}[\boldsymbol{B}^H(\boldsymbol{h})\,\widetilde{\boldsymbol{E}}_d] = \underbrace{\left[\widetilde{\boldsymbol{E}}^{(1)} + \widetilde{\boldsymbol{E}}^{(2)},\ j\left(\widetilde{\boldsymbol{E}}^{(2)} - \widetilde{\boldsymbol{E}}^{(1)}\right)\right]}_{\widetilde{\boldsymbol{P}} \in \mathbb{C}^{M^2\times 2(L_{\text{est}}+1)}} \underbrace{\begin{bmatrix} \boldsymbol{h}_R \\ \boldsymbol{h}_I \end{bmatrix}}_{\widetilde{\boldsymbol{h}} \in \mathbb{R}^{2(L_{\text{est}}+1)}} = \widetilde{\boldsymbol{P}}\,\widetilde{\boldsymbol{h}} \quad (35)$$

and hence the orthogonality condition (33) can be reformulated as $\widetilde{\boldsymbol{P}}\,\widetilde{\boldsymbol{h}} = \mathbf{0}_{2(L_{\text{est}}+1)}$, i.e., as a linear homogeneous system in $\widetilde{\boldsymbol{h}}$. Since, in practice, the autocorrelation matrix $\boldsymbol{R_{zz}}$, and hence $\widetilde{\boldsymbol{P}}$, is estimated from received data, the previous equation does not hold exactly; in this case, it must be solved in the least-square sense as follows

$$\min_{\|\widetilde{\boldsymbol{h}}\|=1} \|\widetilde{\boldsymbol{P}}\,\widetilde{\boldsymbol{h}}\|^2 = \min_{\|\widetilde{\boldsymbol{h}}\|=1} \widetilde{\boldsymbol{h}}^H \widetilde{\boldsymbol{P}}^H \widetilde{\boldsymbol{P}}\,\widetilde{\boldsymbol{h}}\,, \quad (36)$$

where the unit-norm constraint $\|\widetilde{\boldsymbol{h}}\| = 1$ is set to avoid the trivial solution $\widetilde{\boldsymbol{h}} = \mathbf{0}_{2(L_{\text{est}}+1)}$. The solution of (36), according to the Rayleigh-Ritz theorem [15], is given by the eigenvector corresponding to the smallest eigenvalue of $\widetilde{\boldsymbol{P}}^H\widetilde{\boldsymbol{P}}$.

[5]This kind of symmetry contemplates as a particular case channels with zeros exactly on the unit circle, which may or may not be located on the subcarriers. More precisely, observe that when such zeros are located on the subcarriers, the proof of Theorem 1 does not hold, since in this case the matrix $\boldsymbol{B}(\boldsymbol{h})$ loses rank.

A. Extension to the case of NBI

The identification algorithm presented in Section V has been derived in the case of white disturbance, and can be easily generalized, following the derivations of [19, App. C], to accommodate the case of NBI, with known autocorrelation matrix, by whitening the received signal or, equivalently, by resorting to the generalized eigenvalue decomposition (EVD) of the two matrices $\boldsymbol{R_{zz}}$ and $\boldsymbol{R_{dd}}$. In many cases, however, exact knowledge of the NBI autocorrelation matrix is not available, but one might have only partial knowledge about its spectral properties (e.g. its bandwidth). More precisely, due to its narrowband nature, the autocorrelation matrix of the NBI can be accurately approximated by a low-rank matrix, whose rank is related to the NBI bandwidth [1]. On the basis of the (approximate) low-rank characterization of the NBI, we present here a simple extension of the proposed channel identification algorithm, which does not require knowledge of the NBI autocorrelation matrix.

Let us start writing the overall augmented disturbance $\boldsymbol{d}(n)$ in (20) as $\boldsymbol{d}(n) = \boldsymbol{q}(n) + \boldsymbol{w}(n)$, where $\boldsymbol{w}(n)$ is due to white noise with power σ_w^2, and $\boldsymbol{q}(n)$ accounts for the NBI, which is uncorrelated with $\boldsymbol{w}(n)$. To simplify our derivations, let us assume that $\boldsymbol{R_{qq}} \triangleq \mathrm{E}[\boldsymbol{q}(n)\,\boldsymbol{q}^H(n)] \in \mathbb{C}^{2M\times 2M}$ is *exactly* low-rank, with $\text{rank}(\boldsymbol{R_{qq}}) \triangleq r \leq M$. In practice, $r \ll M$ since, compared to the bandwidth of the multicarrier system, the bandwidth of the NBI is small. Because $\boldsymbol{R_{qq}}$ is Hermitian and positive semidefinite, there exists a full-column rank matrix $\boldsymbol{\Gamma} \in \mathbb{C}^{2M\times r}$ such that $\boldsymbol{R_{qq}} = \boldsymbol{\Gamma}\,\boldsymbol{\Gamma}^H$. Thus, (31) can be rewritten as

$$\boldsymbol{R_{zz}} = \sigma_s^2\,\boldsymbol{\mathcal{F}}_0\,\boldsymbol{\mathcal{F}}_0^H + \boldsymbol{R_{qq}} + \sigma_w^2\,\mathbf{I}_{2M} = \boldsymbol{\mathcal{C}}\,\boldsymbol{\mathcal{C}}^H + \sigma_w^2\,\mathbf{I}_{2M}\,, \quad (37)$$

where $\boldsymbol{\mathcal{C}} \triangleq [\sigma_s\,\boldsymbol{\mathcal{F}}_0, \boldsymbol{\Gamma}] \in \mathbb{C}^{2M\times(M+r)}$. In the sequel, we assume that $\boldsymbol{\mathcal{C}}$ is full-column rank, which implies [1] that the two subspaces $\text{range}(\boldsymbol{\mathcal{F}}_0)$ and $\text{range}(\boldsymbol{\Gamma})$ intersect only trivially, i.e., $\text{range}(\boldsymbol{\mathcal{F}}_0) \cap \text{range}(\boldsymbol{\Gamma}) = \{\mathbf{0}_{2M}\}$. Note that, as discussed in [1], the previous one is a condition less restrictive than simple orthogonality between the same subspaces. Since $\text{rank}(\boldsymbol{\mathcal{C}}) = M + r$, the smallest $M - r$ eigenvalues of $\boldsymbol{R_{zz}}$ are equal to σ_w^2, i.e., $\lambda_i = \sigma_w^2$ for $i = M+r, M+r+1, \ldots, 2M-1$. Thus, let $\boldsymbol{E}'_d = [\boldsymbol{e}_{M+r}, \boldsymbol{e}_{M+r+1}, \ldots, \boldsymbol{e}_{2M-1}] \in \mathbb{C}^{2M\times(M-r)}$ contain the corresponding eigenvectors, one has $(\boldsymbol{E}'_d)^H\,\boldsymbol{\mathcal{C}} = \mathbf{O}_{(M-r)\times(M-r)}$. Taking into account the structure of $\boldsymbol{\mathcal{C}}$, the previous relation can be rewritten as

$$\begin{cases} (\boldsymbol{E}'_d)^H\boldsymbol{\mathcal{F}}_0 = \mathbf{O}_{(M-r)\times M}\,, \\ (\boldsymbol{E}'_d)^H\boldsymbol{\Gamma} = \mathbf{O}_{(M-r)\times r}\,. \end{cases} \quad (38)$$

In order to estimate the channel, only the first relation is needed, which is similar to (32); as a matter of fact, all the results based on (32) apply also to this case, including Theorem 1. Furthermore, it should be observed that, in principle, the second relation in (38) would allow one to devise a procedure for identifying the interference parameters: this point, however, is not pursued further, since we do not make any specific assumption regarding interference structure. As a final point, note that, apart from special cases, a narrowband interference does *not* present a matrix $\boldsymbol{R_{qq}}$ which is exactly low-rank. In practice, however, due to the narrowband nature of $\boldsymbol{q}(n)$, only a limited number r_{est} of eigenvalues of $\boldsymbol{R_{qq}}$ are

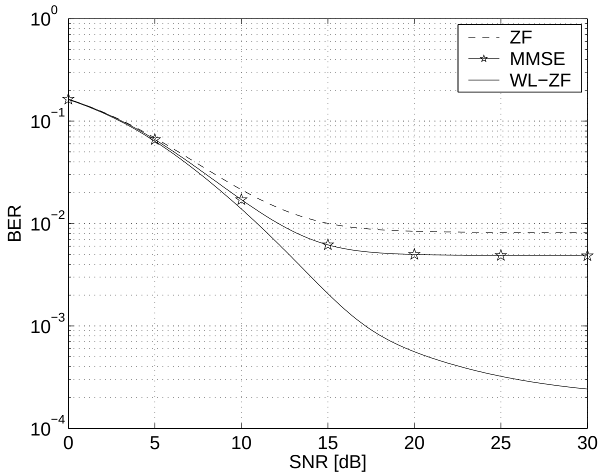

Fig. 1. Average BER versus SNR (SIR = 10 dB, non-blind receivers).

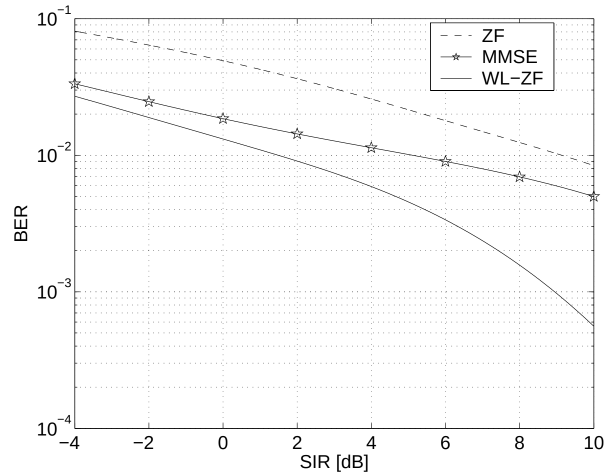

Fig. 2. Average BER versus SIR (SNR = 20 dB, non-blind receivers).

significantly different from zero, and the same considerations can be repeated with reference to the *effective* rank r_{est} of $\boldsymbol{R_{qq}}$, instead of r. Obviously, in this case a modeling error occurs, whose impact on the identification performance is evaluated by simulations in Section VI, turning out to be negligible in practice.

VI. SIMULATION RESULTS

In all the simulations, unless otherwise specified, we consider the following scenario: a multicarrier OFDM system employing $M = 32$ subcarriers with OQPSK signaling and a CP of length $L_{\text{cp}} = 8$, which operates over a nonminimum-phase FIR channel of order $L = 4$ modeled as in [30], i.e., with zeros at $(1.2, -1.2, j\,0.7, -j\,0.7)$. The discrete-time NBI is modeled as a zero-mean WSS circular Gaussian process, with autocorrelation function $r_{\text{NBI}}(m) = \sigma^2_{\text{NBI}}\, a^{|m|}\, e^{j2\pi m\nu_0}$, where σ^2_{NBI} is the NBI power, a can be related to the 3-dB NBI bandwidth ν_3 by $\nu_3 = (2\pi)^{-1} \arccos\left(\frac{4a-a^2-1}{2a}\right)$, $0.172 \leq a < 1$, and ν_0 is the NBI carrier frequency-offset. The discrete-time additive noise is modeled as a zero-mean WSS circular white Gaussian process with power σ^2_w. The SNR (defined as σ^2_s/σ^2_w) is set to 20 dB; the SIR (defined as $\sigma^2_s/\sigma^2_{\text{NBI}}$) is set to 10 dB; the parameters a and ν_0 are set to 0.99 (corresponding to $\nu_3 \approx 0.05/M$) and 4.5$/M$, respectively.

Example 1 – Non-blind equalization performance: As global performance measure for equalization, we adopt the average bit-error rate (BER), defined as $\text{BER} \triangleq M^{-1} \sum_{m=0}^{M-1} \text{BER}^{(m)}$, where $\text{BER}^{(m)}$ is the bit-error rate relative to the mth subcarrier. In the considered scenario wherein the overall disturbance (noise-plus-NBI) is Gaussian-distributed, *exact* BER evaluation can be carried out for both the proposed WL-ZF MOE receiver and the linear ZF one, working under ideal conditions, i.e., perfect knowledge of the channel and, for the WL-ZF MOE receiver, of the autocorrelation matrix $\boldsymbol{R_{zz}}$. Under the same ideal conditions, theoretical BER evaluation can be carried out also for the linear MMSE equalizer, by modeling the residual ICI at its output as a Gaussian additive process. In Fig. 1, we show the average BER as a function of SNR ranging from 0 to 30 dB: the results show that, as the SNR increases, the WL-ZF receiver largely outperforms both the linear ZF and MMSE ones.

Note that the performances of the linear receivers exhibit marked BER floors due to the presence of the NBI, which becomes the predominant source of performance degradation as the SNR increases, while the SIR is kept constant. Results not reported here show that, for values of SNR exceeding 30 dB, also the WL-ZF receiver exhibits a BER floor, albeit at much lower values of BER (around $2 \cdot 10^{-4}$), since its NBI suppression capability is not complete. Fig. 2 shows the average BER curve sketched as a function of SIR, ranging from -4 dB to 10 dB. Compared with ZF and MMSE, the WL-ZF receiver provides again a significant performance gain, which furthermore increases as the SIR increases; for values of SIR exceeding 25 dB (not shown in the figure), however, all the receivers exhibit the same very small BER floor (around $7 \cdot 10^{-7}$), due to the presence of the residual thermal noise. In Fig. 3 the average BER is evaluated as a function of the NBI frequency offset ν_0, normalized to $1/M$, which is the discrete-time OFDM intercarrier spacing. Observe that for all the receivers, and particularly for the WL-ZF one, the performances are better for values of $\nu_0 M \approx 4$. This is due to the fact that, for such a value of $\nu_0 M$, the NBI affects primarily the subcarriers that are less attenuated by the considered frequency-selective channel. Moreover, if we restrict attention to values of $\nu_0 M$ between two adjacent subcarriers, we observe that, unlike the ZF and MMSE receivers, the performance of the WL-ZF receiver is very sensitive to the actual value of $\nu_0 M$. In particular, the performance advantage of the WL-ZF receiver is maximum when the NBI is placed half-way two consecutive subcarriers. Instead, when the NBI is located exactly in correspondence of a subcarrier frequency, the performance of the WL-ZF equalizer is close to that of ZF and MMSE receivers. In fact, in the latter case, the SINR at the input of the equalizer is so low in correspondence of the subcarrier hit by the NBI that the SINR gain of these filters does not translate in a valuable BER improvement. In this case, performance can be improved by resorting to

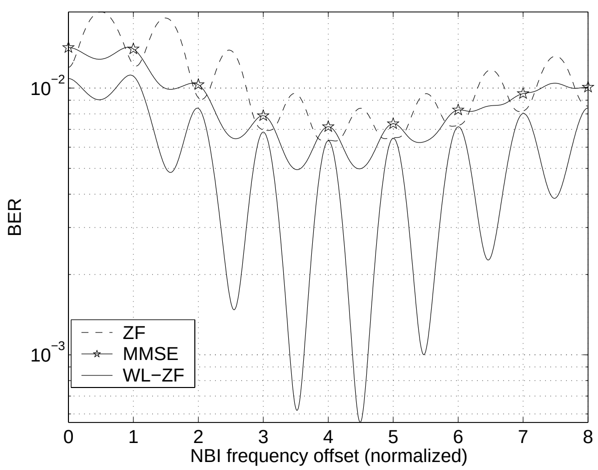

Fig. 3. Average BER versus NBI frequency offset (SNR = 20 dB, SIR = 10 dB, non-blind receivers).

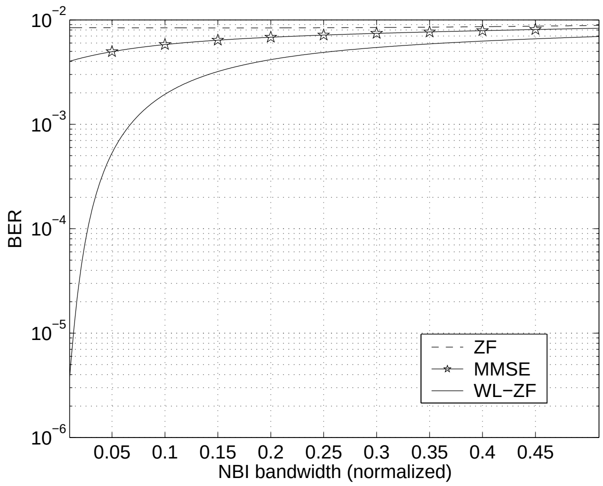

Fig. 4. Average BER versus NBI bandwidth (SNR = 20 dB, SIR = 10 dB, non-blind receivers).

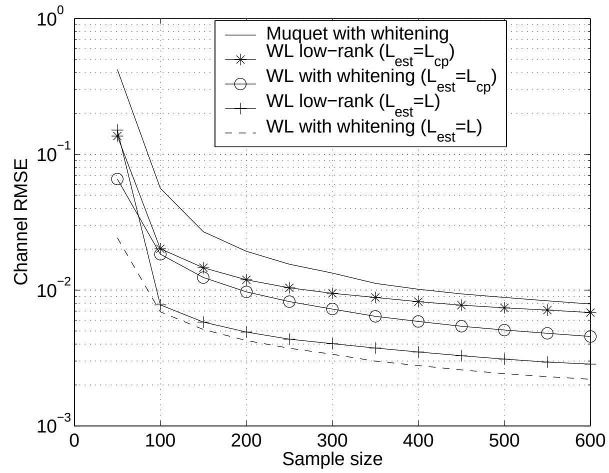

Fig. 5. Channel RMSE versus sample size (SNR = 20 dB, SIR = 10 dB).

channel coding across the subcarriers. When, instead, the NBI is between two subcarriers, the input SINR in correspondence of such subcarriers is only moderately low. Hence, the filters can assure a valuable SINR gain on these subcarriers which, in its turn, translates in a significant BER improvement. In Fig. 4 we show the average BER as a function of the 3-dB NBI bandwidth ν_3, normalized to $1/M$. We note that the WL-ZF performance degrades with increasing values of the NBI bandwidth: in this case, a larger number of subcarriers is corrupted by NBI, and even though the per-carrier SIR increases (the overall SIR is kept constant), the combined effect results in BER degradation.

Example 2 – Blind channel identification performance: To evaluate the channel estimation error, we adopt the normalized root mean-squared error (RMSE), defined according to [27], [26] as RMSE $\triangleq \frac{1}{\|\boldsymbol{h}\|}\sqrt{\frac{1}{(L+1)N_\text{t}}\sum_{p=1}^{N_\text{t}}\|\hat{\boldsymbol{h}}_p-\boldsymbol{h}\|^2}$, where the subscript p refers to the pth Monte Carlo trial and N_t denotes the number of trials, which is fixed to $N_\text{t}=1000$. To resolve the scalar ambiguity inherent to blind channel estimation, the true channel vector $\boldsymbol{h}$ is assumed to be unit-norm and the estimate $\hat{\boldsymbol{h}}_p$ is similarly normalized. To resolve the residual phase ambiguity, we proceed as in [27], [26] by determining the phase of $h(0)/\hat{h}_p(0)$ and compensating the phase of the other estimated channel coefficients prior to RMSE computation. To cope with the colored disturbance environment, we considered two different versions of our blind identification method: the former (WL with whitening in the plots) performs preliminary whitening of the received signal by assuming *perfect* knowledge of the disturbance correlation matrix; the latter (WL low-rank in the plots) resorts to the low-rank approximation described in Section V-A, with the effective rank set to $r_\text{est}=5$. Both versions are tested by assuming either that the estimated channel order L_est is equal to the true one L, or that the channel order is maximally overestimated, i.e., $L_\text{est}=L_\text{cp}$, and compared with the method of Muquet *et al.*, implemented as described in [21] via perfect whitening and for $L_\text{est}=L_\text{cp}$. In Fig. 5 we depict the channel RMSE as a function of the sample size (expressed in number of OFDM symbols). The results show that WL with whitening exhibits the best performance among all techniques, but WL low-rank is competitive when $L_\text{est}=L$ without requiring knowledge of the disturbance autocorrelation matrix, but only an estimate of its rank. The performances of both versions of the proposed method degrade when $L_\text{est}=L_\text{cp}$, nevertheless they remain uniformly better than those of Muquet *et al.* for all considered values of the sample size. Similar considerations apply to Figs. 6 and 7, where the performances are depicted as a function of SNR and SIR, respectively, for a sample size of 500 OFDM symbols. It is shown here that the WL low-rank technique, which does not require knowledge of the disturbance autocorrelation matrix, exhibits performances comparable or superior than those of the method of Muquet *et al.*, and very close to those achieved by WL with whitening, especially when $L_\text{est}=L$. Furthermore, it can be seen that, even though the proposed method is able to work also when the channel order is overestimated, knowledge or estimation of the channel order assures in practice a valuable performance improvement.

Example 3 – Sensitivity to zero positions in blind channel

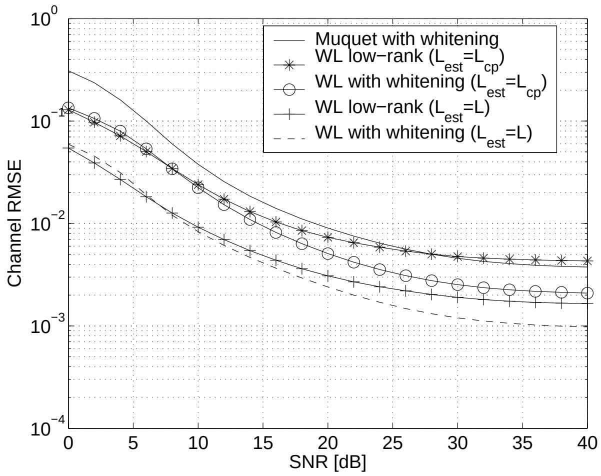

Fig. 6. Channel RMSE versus SNR (SIR = 10 dB, 500 OFDM symbols).

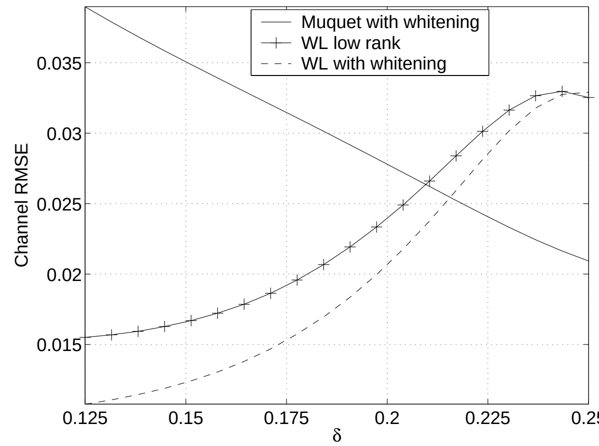

Fig. 8. Channel RMSE versus zero perturbation δ (SNR = 20 dB, SIR = 10 dB).

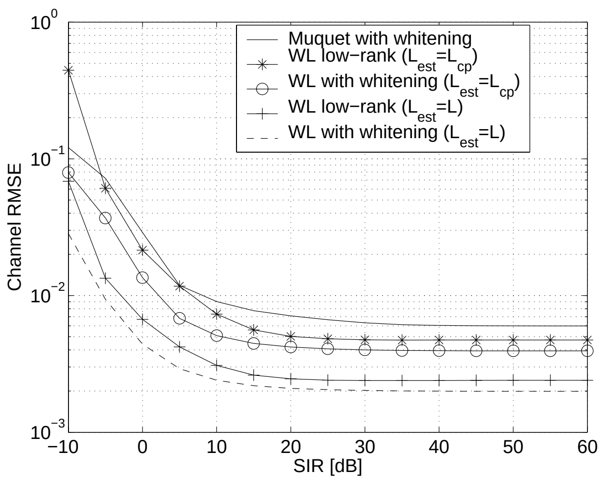

Fig. 7. Channel RMSE versus SIR (SNR = 20 dB, 500 OFDM symbols).

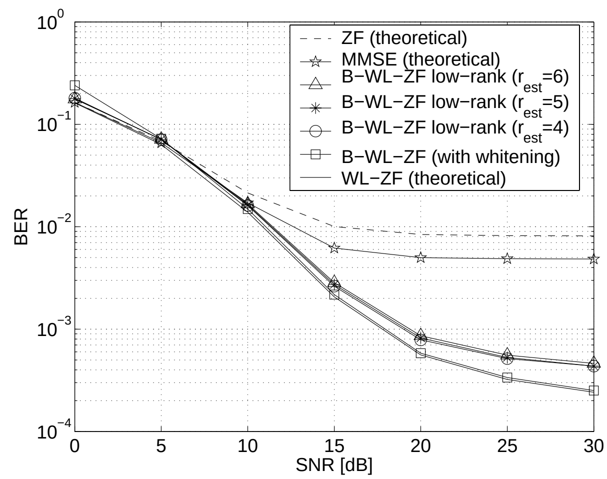

Fig. 9. Average BER versus SNR (SIR = 10 dB, blind receivers).

identification: In this simulation, we show the robustness of the WL blind channel identification algorithm when the channel comes close to being non-identifiable. More specifically, we considered a nonminimum-phase FIR channel of order $L = 4$, with zeros at $(1.2, -1.2, j\,0.7, \frac{1}{0.7}\,e^{j2\pi\delta})$; note that the position of the last zero is parameterized by δ, and for $\delta = 1/4$ the channel is not identifiable according to Theorem 1. In Fig. 8 we depict the channel RMSE evaluated over $N_{\text{t}} = 1000$ Monte Carlo trials and for a sample size of 500 OFDM symbols, as a function of δ in the range $[1/8, 1/4]$. Both versions of the proposed method are still able to outperform the method of Muquet *et al.* for values of $\delta < 0.21$. whereas for higher values of δ their performances degrade, remaining however close to those of Muquet *et al.*.

Example 4 – Blind equalization performance: In this simulation, we evaluate the BER performance of the proposed WL-ZF MOE receiver implemented in a blind manner, i.e., by estimating the channel via the WL algorithm described in Section V and evaluating the matrix $\boldsymbol{R_{zz}}$ from received data, with a sample size of 500 OFDM symbols. After estimating the receiver weights, an independent record of 10^6 OFDM symbols is considered to evaluate the BER. We consider the subspace-based version[6] of the blind WL-ZF MOE receiver, which is implemented either by whitening the received data (referred to as B-WL-ZF with whitening in the plots), or by resorting to an approximate low-rank subspace decomposition (referred to as B-WL-ZF low-rank in the plots) similar to that described for channel identification purposes in Section V-A. Moreover, to show that the low-rank procedure is robust to rank determination, the latter receiver is implemented for three different values of the effective rank, i.e., $r_{\text{est}} = 4, 5, 6$. In Fig. 9, we show the average BER as a function of SNR ranging from 0 dB to 30 dB; to allow for a better comparison, we also depict the theoretical performances of the non-blind receivers already considered in Fig. 1. All the WL receivers significantly outperform the linear ZF and MMSE ones: in particular, the B-WL-ZF with whitening approaches the performance of the non-blind WL-ZF, requiring however perfect knowledge of the disturbance autocorrelation matrix. Instead, the B-WL-ZF low rank receiver incurs only a small performance penalty and,

[6]It is well known that when the MMSE or MOE receivers are estimated from data, a significant gap with respect to ideal performances arises, especially at high SNR, which can however be counteracted in large part by resorting to subspace-based implementation [37].

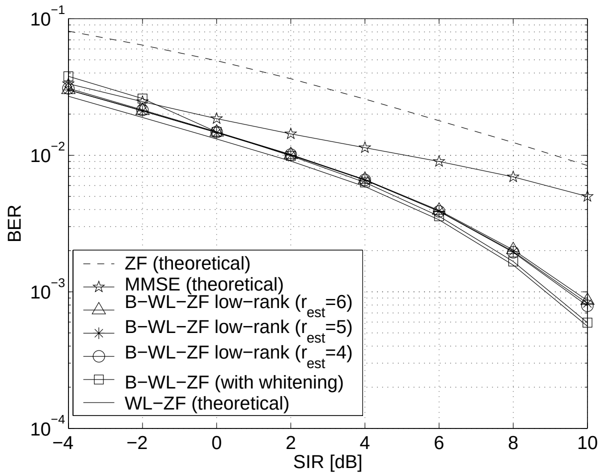

Fig. 10. Average BER versus SIR (SNR = 20 dB, blind receivers).

moreover, its performance is fairly insensitive to the value of r_{est}. Similar considerations apply to Fig. 10, where the average BER is shown as a function of SIR ranging from -4 dB to 10 dB, which again shows that the blind implementations of the WL-ZF receiver can perform very close to their theoretical non-blind limit.

VII. Conclusions

In this paper, we proposed new equalization and blind channel identification techniques for multicarrier systems operating in the presence of possibly strong NBI. In order to exploit the noncircularity property of the signal constellation, we applied the WL approach to the synthesis of ZF equalizers, which jointly elaborate the received signal and its complex conjugate version, gaining thus the degrees of freedom needed to perform NBI suppression. The blind channel identification technique, which exploits the subspace properties of the augmented correlation matrix of the received signal, has been extended to work also in the case of colored interference, without requiring knowledge of the disturbance correlation matrix, but only an estimate of its rank. Compared with the conventional linear ZF and MMSE receivers, the advantage of the MOE WL-ZF receiver is significant when the NBI bandwidth is very small in comparison with the intercarrier spacing and the NBI is not exactly located on a subcarrier.

Appendix I
Proof of Lemma 2

Accounting for (22) and the fact that $\boldsymbol{W}$ is nonsingular, one has $\text{rank}(\boldsymbol{\mathcal{F}}_0) = \text{rank}(\boldsymbol{B}) \leq M$ with $\boldsymbol{B} = [\boldsymbol{\mathcal{H}}^T, \boldsymbol{\mathcal{H}}^H]^T$. Since $\boldsymbol{\mathcal{H}} = \text{diag}[H(0), H(1), \ldots, H(M-1)]$ and $\boldsymbol{\mathcal{H}}^* = \text{diag}[H^*(0), H^*(1), \ldots, H^*(M-1)]$, a necessary and sufficient condition in order for $\boldsymbol{B}$ to be full-rank is $H(k) \neq 0$, $\forall k \in \{0, 1, \ldots, M-1\}$. Indeed, if the previous condition holds, then both $\boldsymbol{\mathcal{H}}$ and $\boldsymbol{\mathcal{H}}$ are nonsingular matrices and hence the rank of $\boldsymbol{B}$ is M. Conversely, if the matrix $\boldsymbol{B}$ is full-rank, let us assume by contradiction that $H(k) = 0$ for one value of k, say $k = \overline{k}$, then the $\overline{k}$-th column of $\boldsymbol{B}$ is zero and, hence, its column-rank degenerates.

Appendix II
Proof of Theorem 1

As a first step toward the proof, we prove the following Lemma.

Lemma 3: Under the assumption that $\boldsymbol{B}(\boldsymbol{h})$ is full-column rank, i.e., $\text{rank}[\boldsymbol{B}(\boldsymbol{h})] = M$, the vector $\boldsymbol{h}'$ is a solution of (33) iff $\text{range}[\boldsymbol{B}(\boldsymbol{h}')] \subseteq \text{range}[\boldsymbol{B}(\boldsymbol{h})]$.

Proof: Let us prove the direct statement. If $\boldsymbol{h}'$ is solution of (33), then $\widetilde{\boldsymbol{E}}_d^H \boldsymbol{B}(\boldsymbol{h}') = \mathbf{O}_{M\times M}$, i.e., each column of $\boldsymbol{B}(\boldsymbol{h}')$ belongs to the orthogonal complement of $\widetilde{\boldsymbol{E}}_d$ and, hence, $\text{range}[\boldsymbol{B}(\boldsymbol{h}')] \subseteq \text{range}^{\perp}(\widetilde{\boldsymbol{E}}_d)$. The same statement holds for $\boldsymbol{B}(\boldsymbol{h})$, i.e., $\text{range}[\boldsymbol{B}(\boldsymbol{h})] \subseteq \text{range}^{\perp}(\widetilde{\boldsymbol{E}}_d)$. Note however that $\widetilde{\boldsymbol{E}}_d = \boldsymbol{W}^H \boldsymbol{E}_d$ in (33) is full-column rank, since $\boldsymbol{E}_d$ is full-column rank (due to linear independence of the noise eigenvectors) and $\boldsymbol{W}$ is nonsingular. Therefore, $\dim[\text{range}^{\perp}(\widetilde{\boldsymbol{E}}_d)] = 2M - \dim[\text{range}(\widetilde{\boldsymbol{E}}_d)] = M$ and, since by assumption $\dim[\text{range}(\boldsymbol{B}(\boldsymbol{h}))] = M$, it turns out that $\text{range}[\boldsymbol{B}(\boldsymbol{h})] = \text{range}^{\perp}(\widetilde{\boldsymbol{E}}_d)$. Thus, $\text{range}[\boldsymbol{B}(\boldsymbol{h}')] \subseteq \text{range}[\boldsymbol{B}(\boldsymbol{h})]$ and this completes the proof of the direct statement. The proof of the inverse statement is easier. If $\text{range}[\boldsymbol{B}(\boldsymbol{h}')] \subseteq \text{range}[\boldsymbol{B}(\boldsymbol{h})]$, the columns of $\boldsymbol{B}(\boldsymbol{h}')$ must belong to $\text{range}[\boldsymbol{B}(\boldsymbol{h})]$ and, hence, be orthogonal to the columns of $\widetilde{\boldsymbol{E}}_d$, which means that $\widetilde{\boldsymbol{E}}_d^H \boldsymbol{B}(\boldsymbol{h}') = \mathbf{O}_{M\times M}$ and, hence, $\boldsymbol{h}'$ is a solution of (33). ■

Accounting for Lemma 3, the proof of Theorem 1 can be equivalently carried out by showing that, under assumptions (i)-(iii), the following two statements are equivalent:

(1′) $\text{range}[\boldsymbol{B}(\boldsymbol{h}')] \subseteq \text{range}[\boldsymbol{B}(\boldsymbol{h})]$.
(2) $\boldsymbol{h}' = \alpha \boldsymbol{h}$, with $\alpha \in \mathbb{R}$.

The inverse implication (2) ⇒ (1′) is easily proven. In fact, if $\boldsymbol{h}' = \alpha \boldsymbol{h}$ with $\alpha \in \mathbb{R}$, it turns out that $\boldsymbol{B}(\boldsymbol{h}') = \alpha\, \boldsymbol{B}(\boldsymbol{h})$ and, hence, $\text{range}[\boldsymbol{B}(\boldsymbol{h}')] = \text{range}[\boldsymbol{B}(\boldsymbol{h})]$.

The only difficulty lies in the direct part (1′) ⇒ (2). If $\text{range}[\boldsymbol{B}(\boldsymbol{h}')] \subseteq \text{range}[\boldsymbol{B}(\boldsymbol{h})]$, then each column of $\boldsymbol{B}(\boldsymbol{h}')$ belongs to $\text{range}[\boldsymbol{B}(\boldsymbol{h})]$ and, hence, it can be expressed as a linear combination of the columns of $\boldsymbol{B}(\boldsymbol{h})$. Thus, there exists a matrix $\boldsymbol{\Psi} \in \mathbb{C}^{M\times M}$ such that $\boldsymbol{B}(\boldsymbol{h}') = \boldsymbol{B}(\boldsymbol{h})\boldsymbol{\Psi}$. By recalling the structure of $\boldsymbol{B}(\boldsymbol{h}')$ and $\boldsymbol{B}(\boldsymbol{h})$, the previous relation is equivalent to

$$\boldsymbol{\mathcal{H}}(\boldsymbol{h}') = \boldsymbol{\mathcal{H}}(\boldsymbol{h})\, \boldsymbol{\Psi}\,, \tag{39}$$

$$\boldsymbol{\mathcal{H}}^*(\boldsymbol{h}') = \boldsymbol{\mathcal{H}}^*(\boldsymbol{h})\, \boldsymbol{\Psi} \tag{40}$$

Since $\boldsymbol{\mathcal{H}}(\boldsymbol{h})$ is nonsingular, we can obtain $\boldsymbol{\Psi}$ from (39) as $\boldsymbol{\Psi} = \boldsymbol{\mathcal{H}}(\boldsymbol{h})^{-1}\boldsymbol{\mathcal{H}}(\boldsymbol{h}')$, which shows that $\boldsymbol{\Psi}$ is a diagonal matrix, since both $\boldsymbol{\mathcal{H}}(\boldsymbol{h}')$ and $\boldsymbol{\mathcal{H}}(\boldsymbol{h})$ are such. Moreover, (39) and (40) show that the entries of $\boldsymbol{\Psi}$ are necessarily *real* numbers. At this point, we can retain only (39), with the additional condition that $\boldsymbol{\Psi}$ is diagonal and real. Note that (39) can be rewritten in scalar terms as $H'(k) = \Psi(k)\, H(k)$, $k \in \{0, 1, \ldots, M-1\}$ with $\Psi(k) \in \mathbb{R}$. If we define $\{\psi(n)\}_{n=0}^{M-1} \triangleq \text{IDFT}[\Psi(k)]$, the product property of the DFT assures that the time-domain counterpart of the previous relation is a circular convolution, which can be written in matrix notation as

$$\boldsymbol{h}'_{\text{zp}} \triangleq \begin{bmatrix} \boldsymbol{h}' \\ \mathbf{0}_{M-L-1} \end{bmatrix}$$

$$= \begin{bmatrix} \psi(0) & \psi(M-1) & \dots & \psi(1) \\ \psi(1) & \psi(0) & \dots & \psi(2) \\ \vdots & \vdots & \vdots & \vdots \\ \psi(M-1) & \psi(M-2) & \dots & \psi(0) \end{bmatrix} \underbrace{\begin{bmatrix} \boldsymbol{h} \\ \boldsymbol{0}_{M-L-1} \end{bmatrix}}_{\boldsymbol{h}_{\text{zp}}}, \tag{41}$$

where $\boldsymbol{h}_{\text{zp}} \in \mathbb{C}^M$ and $\boldsymbol{h}'_{\text{zp}} \in \mathbb{C}^M$ are obtained from $\boldsymbol{h} \in \mathbb{C}^{L+1}$ and $\boldsymbol{h}' \in \mathbb{C}^{L+1}$ by padding of $M-L-1$ zeros (note that by assumption (ii) $M \geq 2L+1$ and hence $M-L-1 \geq L > 0$). Since the circular convolution obeys the commutative property, (41) can also be written as

$$\boldsymbol{h}'_{\text{zp}} = \boldsymbol{H}\boldsymbol{\psi} = \boldsymbol{H} \begin{bmatrix} \psi(0) \\ \widetilde{\boldsymbol{\psi}} \end{bmatrix}, \tag{42}$$

where $\boldsymbol{H} \in \mathbb{C}^{M \times M}$ is the circulant matrix having $\boldsymbol{h}_{\text{zp}}$ as its first column, $\boldsymbol{\psi} \triangleq [\psi(0), \psi(1), \dots, \psi(M-1)]^T$ and $\widetilde{\boldsymbol{\psi}} \triangleq [\psi(1), \psi(2), \dots, \psi(M-1)]^T$. Since the M-sequence $\psi(n)$ has a *real* DFT, it must be conjugate symmetric, i.e., $\psi(n) = \psi^*[(M-n)_M]$, $n = 0, 1, \dots, M-1$, with $(\cdot)_M$ denoting the modulo-M operation. Therefore, in (42) $\psi(0)$ must be real, and $\widetilde{\boldsymbol{\psi}}$ must obey the symmetry relation $\widetilde{\boldsymbol{\psi}}^* = \boldsymbol{J}\,\widetilde{\boldsymbol{\psi}}$, with $\boldsymbol{J} \in \mathbb{R}^{(M-1)\times(M-1)}$ representing the backward identity permutation matrix [15], whose elements are defined as $\{\boldsymbol{J}\}_{ij} = \delta_{i+j-M+1}$, $i, j \in \{0, 1, \dots, M-1\}$. Let us rewrite (42) by partitioning $\boldsymbol{H}$ accordingly to $\boldsymbol{h}'_{\text{zp}}$:

$$\boldsymbol{h}'_{\text{zp}} = \begin{bmatrix} \boldsymbol{h}' \\ \boldsymbol{0}_{M-L-1} \end{bmatrix} = \begin{bmatrix} \boldsymbol{H}_1 \\ \boldsymbol{H}_2 \end{bmatrix} \boldsymbol{\psi}, \tag{43}$$

where $\boldsymbol{H}_1 \in \mathbb{C}^{(L+1)\times M}$ and $\boldsymbol{H}_2 \in \mathbb{C}^{(M-L-1)\times M}$; it follows that

$$\boldsymbol{h}' = \boldsymbol{H}_1\boldsymbol{\psi} \quad \text{and} \quad \boldsymbol{0}_{M-L-1} = \boldsymbol{H}_2\boldsymbol{\psi}. \tag{44}$$

Since by hypothesis the channel $h(n) \equiv 0$ for $n = L+1, L+2, \dots, M$, it turns out that the first column of matrix $\boldsymbol{H}_2$ is zero and, hence, $\boldsymbol{H}_2 = [\boldsymbol{0}_{M-L-1}, \overline{\boldsymbol{H}}_2]$, with $\overline{\boldsymbol{H}}_2 \in \mathbb{C}^{(M-L-1)\times(M-1)}$. Taking into account the partitioning of $\boldsymbol{\psi}$ as in (42), the second relation in (44) can be rewritten as

$$\boldsymbol{0}_{M-L-1} = [\boldsymbol{0}_{M-L-1}, \overline{\boldsymbol{H}}_2] \begin{bmatrix} \psi(0) \\ \widetilde{\boldsymbol{\psi}} \end{bmatrix} = \overline{\boldsymbol{H}}_2 \widetilde{\boldsymbol{\psi}}, \tag{45}$$

with

$$\overline{\boldsymbol{H}}_2 = \begin{bmatrix} h(L) & h(L-1) & \dots & h(0) & \dots & \dots & 0 \\ 0 & h(L) & \dots & h(1) & h(0) & \dots & 0 \\ \vdots & \vdots & \vdots & \vdots & \vdots & \vdots & \vdots \\ 0 & 0 & \dots & h(L) & \dots & \dots & h(0) \end{bmatrix}. \tag{46}$$

In order to take into account the conjugate symmetry of $\widetilde{\boldsymbol{\psi}}$, the complex conjugate of (45) must be considered as an additional equation

$$\boldsymbol{0}_{M-L-1} = \overline{\boldsymbol{H}}_2^* \widetilde{\boldsymbol{\psi}}^* = \overline{\boldsymbol{H}}_2^* \boldsymbol{J}\,\widetilde{\boldsymbol{\psi}}. \tag{47}$$

Thus, by stacking (45) and (47) we obtain the following homogeneous system:

$$\boldsymbol{0}_{2(M-L-1)} = \underbrace{\begin{bmatrix} \overline{\boldsymbol{H}}_2 \\ \overline{\boldsymbol{H}}_2^* \boldsymbol{J} \end{bmatrix}}_{\boldsymbol{P}} \widetilde{\boldsymbol{\psi}}, \tag{48}$$

with $\boldsymbol{P} \in \mathbb{C}^{2(M-L-1)\times(M-1)}$. The key point is to show that system (48) admits only the trivial solution $\widetilde{\boldsymbol{\psi}} = \boldsymbol{0}_{M-1}$, in which case (41) yields $\boldsymbol{h}' = \alpha\,\boldsymbol{h}$, with $\alpha = \psi(0) \in \mathbb{R}$. This is equivalent to show that matrix $\boldsymbol{P}$ is full-column rank. Hence, a necessary condition is that $M-1 \leq 2(M-L-1)$, i.e., $M \geq 2\,L+1$, which is assumption (ii). Under this assumption, note that after a row permutation (which does not affect the column rank properties) and taking into account the properties of $\boldsymbol{J}$, matrix $\boldsymbol{P}$ can be written as

$$\boldsymbol{P}' = \begin{bmatrix} h(L) & h(L-1) & \dots & h(0) & \dots & \dots & 0 \\ h^*(0) & h^*(1) & \dots & h^*(L) & \dots & \dots & 0 \\ 0 & h(L) & \dots & h(1) & h(0) & \dots & 0 \\ 0 & h^*(0) & \dots & h^*(L-1) & h^*(L) & \dots & 0 \\ \vdots & \vdots & \vdots & \vdots & \vdots & \vdots & \vdots \\ 0 & 0 & \dots & h(L) & \dots & \dots & h(0) \\ 0 & 0 & \dots & h^*(0) & \dots & \dots & h^*(L) \end{bmatrix}. \tag{49}$$

Finally, observe that $\boldsymbol{P}'$ has the typical block Sylvester structure arising in single-carrier subspace-based blind channel identification, hence we can apply standard results (e.g., [19], [32]) to characterize its rank properties. Specifically, if we evaluate the z-transforms of the first and second row of $\boldsymbol{P}'$, respectively, as $H_1(z) = \sum_{\ell=0}^{L} h(L-\ell)\,z^{-\ell}$ and $H_2(z) = \sum_{\ell=0}^{L} h^*(\ell)\,z^{-\ell} = [\sum_{\ell=0}^{L} h(\ell)\,(z^*)^{-\ell}]^* = H^*(z^*)$, we can invoke [32, Theorem 1 and Corollary 2] to support the following claim:[7] *the matrix $\boldsymbol{P}'$ is full-column rank iff the polynomials $H_1(z)$ and $H_2(z)$ are coprime, i.e., they do not have common zeros.* Note that since by straightforward manipulations it turns out that

$$H_1(z) = H_2^*\left(\frac{1}{z^*}\right) z^{-L}, \tag{50}$$

then, if $z_0 \neq 0$ is a zero common to $H_1(z)$ and $H_2(z)$, we have:

$$H_1(z_0) = H_2^*\left(\frac{1}{z_0^*}\right) z_0^{-L} = H_2(z_0) = 0, \tag{51}$$

and hence z_0 and $1/z_0^*$ are both zeros of $H_2(z)$, i.e., z_0^* and $1/z_0$ are both zeros of $H(z)$. Hence, matrix $\boldsymbol{P}'$ is full-column rank iff the channel transfer function $H(z)$ does not have zeros exhibiting the symmetry of (iii).

ACKNOWLEDGMENTS

The authors would like to thank the anonymous reviewers for their stimulating and detailed comments, which helped improve the quality and presentation of the paper.

REFERENCES

[1] R.T. Behrens and L.L. Scharf, "Signal processing applications of oblique projection operators," *IEEE Trans. Signal Processing*, vol. 42, pp. 1413–1424, June 1994.

[2] W. A. Brown, "On the theory of cyclostationary signals," Ph.D. dissertation, Dep. Elec. Eng. Comput. Sci., Univ. California, Davis, 1987.

[7] Note that at least one of the polynomials $H_1(z)$ and $H_2(z)$ has maximal order L, since, by assumption A3, $h(0), h(L) \neq 0$. This statement continues to hold also when the channel order is overestimated, because $h(L_{\text{cp}}) \neq 0$ might not be true, but surely $h(0) \neq 0$ in this case.

[3] W. M. Brown and R. B. Crane "Conjugate linear filtering," *IEEE Trans. Inform. Theory*, vol. IT–15, pp. 462–465, July 1969.

[4] P. Ciblat, E. Serpedin, and Y. Wang, "On a blind fractionally sampling-based carrier frequency offset estimator for noncircular transmissions," *IEEE Signal Processing Lett.*, vol. 10, pp. 89–92, Apr. 2003.

[5] P. Ciblat and L. Vandendorpe, "Blind carrier frequency offset estimation for noncircular constellation-based transmissions," *IEEE Trans. Signal Processing*, vol. 51, pp. 1378–1389, May 2003.

[6] D. Darsena, G. Gelli, L. Paura, F. Verde, "Widely linear subspace-based blind identification of SISO FIR systems with improper random inputs", in *Proc. of 6th Baiona Workshop on Signal Processing in Communications*, Baiona (Spain), September 2003, pp. 109–114.

[7] D. Darsena, G. Gelli, L. Paura, and F. Verde, "Joint equalisation and interference suppression in OFDM systems," *Electronics Letters*, vol. 39, pp. 873–874, May 2003.

[8] G. Gelli and F. Verde, "Two-stage interference-resistant adaptive periodically time-varying CMA blind equalization," *IEEE Trans. Signal Processing*, vol. 50, pp. 662–672, Mar. 2002.

[9] G. Gelli, L. Paura, and A. M. Tulino, "Cyclostationarity-based filtering for narrowband interference suppression in direct-sequence spread-spectrum systems," *IEEE J. Select. Areas Commun.*, vol. 16, pp. 1747–1755, Dec. 1998.

[10] G. Gelli, L. Paura, and A. R. P. Ragozini, "Blind widely linear multiuser detection," *IEEE Commun. Lett.*, vol. 4, pp. 187–189, June 2000.

[11] W.H. Gerstacker, R. Schober and A. Lampe, "Receivers with widely linear processing for frequency-selective channels," *IEEE Trans. Commun.*, vol. 51, no. 9, pp. 1512–1523, Sept. 2003.

[12] W. Gerstacker, F. Obernosterer, R. Schober, A. Lehmann, A. Lampe, and P. Gunreben, "Widely linear equalization of space-time block-coded transmission over fading ISI channels," in *Proc. of VTC Fall 2002*, Vancouver (Canada), September 2002, pp. 238–242.

[13] L. J. Griffiths and C. W. Jim, "An alternative approach to linearly constrained adaptive beamforming," *IEEE Trans. Antennas and Propagat.*, vol. 30, pp. 27–34, Jan. 1982.

[14] M. Honig, U. Madhow, and S. Verdú, "Blind adaptive multiuser detection," *IEEE Trans. Inform. Theory*, vol. 41, pp. 944–960, July 1995.

[15] R. A. Horn and C. R. Johnson. *Matrix analysis*. Cambridge University Press, 1990.

[16] A. Lampe, R. Schober, W. Gerstacker, and J. Huber, "A novel iterative multiuser detector for complex modulation schemes," *IEEE J. Select. Areas Commun.*, vol. 20, pp. 339–350, Feb. 2002.

[17] Y. Li and N. R. Sollenberger, "Adaptive antenna arrays for OFDM systems with co-channel interference," *IEEE Trans. Commun.*, vol. 47, pp. 217–229, Feb. 1999.

[18] S. H. Müller-Weinfurtner, "Optimum Nyquist windowing in OFDM receivers," *IEEE Trans. Commun.*, vol. 49, pp. 417–420, Mar. 2002.

[19] E. Moulines, P. Duhamel, J. Cardoso, and S. Mayrargue, "Subspace methods for the blind identification of multichannel FIR filters," *IEEE Trans. Signal Processing*, vol. 43, pp. 516–525, Feb. 1995.

[20] B. Muquet, Z. Wang, G. B. Giannakis, M. de Courville, and P. Duhamel, "Cyclic prefixing of zero padding for wireless multicarrer transmissions?," *IEEE Trans. Commun.*, vol. 50, pp. 2136–2148, Dec. 2002.

[21] B. Muquet, M. de Courville, and P. Duhamel, "Subspace-based blind and semi-blind channel estimation for OFDM systems,", *IEEE Trans. Signal Processing*, vol. 50, pp. 1699–1712, July 2002.

[22] R. Penrose, "A generalized inverse for matrices," *Proceedings of the Cambridge Philosophical Society*, vol. 51, pp. 406–413, 1955.

[23] B. Picinbono, "On circularity," *IEEE Trans. Signal Processing*, vol. 42, pp. 3473–3482, Dec. 1994.

[24] B. Picinbono and P. Chevalier, "Widely linear estimation with complex data," *IEEE Trans. Signal Processing*, vol. 43, pp. 2030–2033, Aug. 1995.

[25] J. G. Proakis. *Digital communications (2nd ed.).* McGraw-Hill, New York, 1989.

[26] S. Roy and C. Li, "A subspace blind channel estimation method for OFDM systems without cyclic prefix," *IEEE Trans. Wireless Commun.*, vol. 1, pp. 572–579, Oct. 2002.

[27] C. Li and S. Roy, "Subspace-based blind channel estimation method for OFDM by exploiting virtual carriers," *IEEE Trans. Wireless Commun.*, vol. 2, pp. 141–150, Jan. 2003.

[28] A. Scaglione, S. Barbarossa, and G. B. Giannakis, "Filterbank transceivers optimizing information rate in block transmission over dispersive channels", *IEEE Trans. Inform. Theory*, vol. 45, no. 3, pp. 1019–1032, Apr. 1999.

[29] A. Scaglione, G. B. Giannakis and S. Barbarossa, "Redundant filterbank precoders and equalizers Part I: unification and optimal designs," *IEEE Trans. Signal Processing*, vol. 47, pp. 1988–2006, July 1999.

[30] A. Scaglione, G. B. Giannakis and S. Barbarossa, "Redundant filterbank precoders and equalizers Part II: blind channel estimation, synchronization and direct equalization," *IEEE Trans. Signal Processing*, vol. 47, pp. 2007–2022, July 1999.

[31] S. V. Schell "A separability theorem for $2M$ conjugate-symmetric signals impinging on an M-element sensor array," *IEEE Trans. Signal Processing*, vol. 45, no. 3, pp. 789–792, Mar. 1997.

[32] E. Serpedin and G. B. Giannakis, "A simple proof of a known blind channel identifiability result," *IEEE Trans. Signal Processing*, vol. 47, no. 2, pp. 591–593, Feb. 1999.

[33] P. Siohan, C. Siclet, and N. Lacaille, "Analysis and design of OFDM/OQAM systems based on filterbank theory," *IEEE Trans. Signal Processing*, vol. 50, no. 5, pp. 1170–1183, May 2002.

[34] Y. C. Yoon and H. Leib, "Maximizing SNR in improper complex noise and applications to CDMA,", *IEEE Commun. Lett.*, vol. 1, pp. 5–8, Jan. 1997.

[35] H. Yang and M.A. Ingram, "Design of partially adaptive arrays using the singular-value decomposition," *IEEE Trans. Antennas Propagat.*, vol. 45, pp. 843–850, May 1997.

[36] Z. Wang and G. B. Giannakis, "Wireless multicarrier communications – Where Fourier meets Shannon," *IEEE Signal Processing Magazine*, vol. 17, no. 3, pp. 29–48, May 2000.

[37] X. Wang and H. V. Poor, "Blind multiuser detection: a subspace approach," *IEEE Trans. Inform. Theory*, vol. 44, pp. 677–690, Mar. 1998.

Donatella Darsena was born in Napoli, Italy, on December 11, 1975. She received the Dr. Eng. degree *summa cum laude* in telecommunications engineering in 2001 from the University of Napoli Federico II. She is currently a Ph.D. student in electronic and telecommunications engineering at the Department of Electronic and Telecommunication Engineering, University of Napoli Federico II.

Her research activities lie in the area of statistical signal processing, digital communications, and communication systems. In particular, her current interests are focused on equalization, channel identification and narrowband-interference suppression for multicarrier systems.

Giacinto Gelli (M'02) was born in Napoli, Italy, on July 29, 1964. He received the Dr. Eng. degree *summa cum laude* in electronic engineering in 1990, and the Ph.D. degree in computer science and electronic engineering in 1994, both from the University of Napoli Federico II.

From 1994 to 1998, he was an Assistant Professor with the Department of Information Engineering, Second University of Napoli. Since 1998, he has been an Associate Professor of Telecommunications with the Department of Electronic and Telecommunication Engineering, University of Napoli Federico II. He also held teaching positions at the University Parthenope, Napoli, Italy. His research interests are in the fields of statistical signal processing, array processing, image processing, and mobile communications, with current emphasis on code-division multiple-access systems and multicarrier modulation.

Luigi Paura was born in Napoli, Italy, on February 20, 1950. He received the Dr. Eng. degree *summa cum laude* in electronic engineering in 1974 from the University of Napoli Federico II.

From 1979 to 1984 he was with the Department of Electronic and Telecommunication Engineering, University of Napoli, Italy, first as an Assistant Professor and then as an Associate Professor. Since 1994, he has been a Full Professor of Telecommunications: first, with the Department of Mathematics, University of Lecce, Italy; then, with the Department of Information Engineering, Second University of Napoli; and, finally, from 1998 he has been with the Department of Electronic and Telecommunication Engineering, University of Napoli Federico II. He also held teaching positions at the University of Salerno, Italy, at the University of Sannio, Italy, and the University Parthenope, Napoli, Italy. In 1985-86 and 1991 he was a Visiting Researcher at the Signal and Image Processing Laboratory, University of California, Davis. At the present time, his research activities are mainly concerned with statistical signal processing, digital communication systems and medium access control in wireless networks.

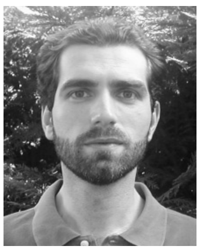

Francesco Verde was born in Santa Maria Capua Vetere, Italy, on June 12, 1974. He received the Dr. Eng. degree *summa cum laude* in electronic engineering in 1998 from the Second University of Napoli, and the Ph.D. degree in information engineering in 2002, from the University of Napoli Federico II.

Since 2002, he has been an Assistant Professor with the Department of Electronic and Telecommunication Engineering, University of Napoli Federico II. His research activities lie in the area of statistical signal processing, digital communications, and communication systems. In particular, his current interests are focused on cyclostationarity-based techniques for blind identification, equalization and interference suppression for narrowband modulation systems, code-division multiple-access systems and multicarrier modulation systems.